

USING POSTMORTEM SHELL AGES TO QUANTIFY POST-
DEPOSITIONAL REWORKING

A Thesis

by

RYAN SAMUELS

Submitted to the Office of Graduate and Professional Studies of
Texas A&M University
in partial fulfillment of the requirements for the degree of

MASTER OF SCIENCE

Chair of Committee,	Ryan C. Ewing
Co-Chair of Committee,	Thomas D. Olszewski
Committee Member,	Timothy M. Dellapenna
Head of Department,	Michael C. Pope

May 2017

Major Subject: Geology

Copyright 2017 Ryan Colburn Samuels

ABSTRACT

This study uses the postmortem ages of *Mulinia lateralis* shells from surface sediments and shallow cores (3-m-long) to quantify net sediment accumulation and reworking rates in the estuary and delta platform of the Aransas River delta, Copano Bay, Texas. The scale of time averaging is governed by two factors: condensation, which determines the minimum possible degree of time averaging in a given increment of stratigraphic thickness, and reworking, which causes further time averaging post-depositionally. The net sediment accumulation rates of the estuary and delta platform are 0.29 mm/yr and 0.73 mm/yr, respectively. In both locations, the top 20 cm of sediment contain a distinct, essentially modern assemblage. Although the estuary is capable of preserving a temporal resolution of ~88 years per 10 cm, shells within 10-cm intervals at depths of 20 to 70 cm have age ranges spanning between 393.92 and 743.89 years. In contrast, the delta platform is capable of preserving a temporal resolution of ~35 years per 10 cm, but shells within 10-cm intervals at depths from 20 to 225 cm have age ranges spanning between 78.37 and 1031.69 years. These results indicate that the rate and depth of reworking, not condensation, primarily govern the magnitude of time averaging in the sediment column of the Aransas River deltaic system as it progrades into Copano Bay.

CONTRIBUTORS AND FUNDING SOURCES

Contributors

This work was supported by a thesis committee consisting of Professors Ryan C. Ewing (Chair) and Thomas D. Olszewski (Co-chair) of the Texas A&M University Department of Geology and Geophysics and Professor Timothy M. DellaPenna of the Texas A&M University at Galveston Department of Oceanography.

All Amino Acid Racemization Analyses and AMS ^{14}C were conducted at the Northern Arizona University Amino Acid Geochronology Laboratory by Dr. Darrell Kaufman and Katherine Whitacre.

All other work conducted for this thesis was completed by Ryan Samuels independently.

Funding Sources

This work was made possible in part by the Petroleum Research Fund of the American Chemical Society under PRF# 54947-ND8 and the American Association of Petroleum Geologists under the 2015 James E. Hooks Memorial Grant.

Its contents are solely the responsibility of the authors and do not necessarily represent the official views of the American Chemical Society or the American Association of Petroleum Geologists.

TABLE OF CONTENTS

	Page
ABSTRACT.....	ii
CONTRIBUTORS AND FUNDING SOURCES	iii
TABLE OF CONTENTS.....	iv
LIST OF TABLES	v
LIST OF FIGURES	vi
1. INTRODUCTION	1
2. BACKGROUND	3
3. SEDIMENTOLOGY	5
3.1 Methods.....	5
3.2 Results.....	6
3.2.1 Core Description	6
3.2.2 Grain Size.....	6
3.2.3 Facies Analysis	7
3.3 Depositional Model.....	12
4. SHELL AGE SPECTRA	13
4.1 Methods.....	13
4.1.1 Sampling	13
4.1.2 Amino Acid Racemization.....	13
4.1.3 Amino Acid Analyses	14
4.1.4 Age Model	15
4.2 Results.....	21
4.2.1 Shell Reliability	21
4.2.2 Shell Ages in the Sediment Column	21
4.2.3 Postmortem Age Spectra in Surface Samples.....	22
5. DISCUSSION	28
6. CONCLUSIONS	31
REFERENCES	32
APPENDIX.....	38

LIST OF TABLES

	Page	
Table 1	Sedimentary facies.....	12
Table 2	Major-axis regression of Glu-based versus Asp-based age estimates	19
Table 3	Summary of AAR chronology by sampled layers	25
Table 4	CB 1-2 grain size distributions vs. depth.....	38
Table 5	CB 2-2 grain size distributions vs. depth.....	56
Table 6	Absolute ^{14}C age data used to fit age-D/L models	71
Table 7	Core CB 1-2 specimens	72
Table 8	Core CB 2-2 specimens	79
Table 9	CB 1-2 surface specimens	85
Table 10	CB 2-2 surface specimens	87

LIST OF FIGURES

	Page
Figure 1 Location and facies map of Copano Bay, Texas	4
Figure 2 Sediment cores, measured sections, and x-rays of CB 1-2 (Top) and CB 2-2 (Bottom)	8
Figure 3 Grain size distribution vs. depth for each core site	10
Figure 4 Glutamic and Aspartic amino acid D/L ratios.....	17
Figure 5 Amino acid age models.....	19
Figure 6 Scatterplot of Glu-based and Asp-based age values	20
Figure 7 Depth vs. postmortem age plots	23
Figure 8 Inferred shell ages with sediment depth for both CB 1-2 (A) and CB 2-2 (B)	26
Figure 9 Surface age spectra for A) CB 1-2 and B) CB 2-2.....	27

1. INTRODUCTION

Determining the chronological framework of deltas is essential for studying the stratigraphic architecture of past and modern deltaic systems (McManus, 2002; Pont et al., 2002; Nilsson et al, 2005). Currently, sedimentary geologists are able to predict the stratigraphic architecture of deltaic deposits and relate it to surface processes. However, post-depositional sediment reworking has remained relatively unconstrained.

Quantifying the extent of post-depositional reworking would allow sedimentary geologists to better understand how such processes affect the stratigraphic architecture of past and modern deltaic systems as they evolve.

In many previous studies of deltaic systems, radiocarbon dating of individual biological specimens (i.e., wood, shell, or bone) was applied to date sediments at depth (Moslow & Heron, 1979; Heron et al., 1984; Thom & Roy, 1985; Kraft et al., 1987; Nichols et al., 1991; Denys & Baeteman, 1995; Davis et al., 2001; Behre, 2004; Chang et al., 2006; Bungenstock & Schäfer, 2009; Tessier et al., 2012). Such single age estimates are important, but they cannot provide information on the degree of time averaging (Cubizolle et al, 2007; Kosnik et al., 2015), which results from mixing the remains of organisms that did not live contemporaneously (e.g., Powell et al. 1992; Flessa et al. 1993; Flessa and Kowalewski 1994; Kowalewski, 1996; Kowalewski et al. 1998; Carroll et al. 2003; Kidwell et al. 2005; Kosnik et al. 2007, 2009; Simonson et al. 2013; Dexter et al. 2014).

Time averaging results from at least two factors: condensation (governed by rate of sediment accumulation) and reworking (governed by the degree of post-depositional

mixing). The rate of sediment accumulation determines the minimum possible degree of time averaging in a given increment of stratigraphic thickness, with higher rates of accumulation necessarily resulting in less time averaging (Meldahl et al, 1997). Post-depositional reworking, either physical or biogenic, causes further time averaging, with deeper and faster sediment mixing leading to more time averaging (Olszewski, 2004).

This study uses the postmortem ages of *Mulinia lateralis* shells from surface sediments and shallow cores to estimate rates of sediment accumulation and reworking in the Aransas River delta system. Dead molluscan shells function as natural tracer particles of sediment grains during deposition and burial because they are produced at the sediment-water interface near their site of deposition and their postmortem ages indicate how long it took for them to reach their final location in the sediment column. The purpose of this study is to use postmortem shell ages to evaluate and compare the accumulation and reworking rates in different settings of a deltaic system.

2. BACKGROUND

Copano Bay (Figure 1) is a shallow (~2-4 meters) microtidal estuary located on the Texas Gulf coast that initially formed ~9600 years ago as a result of Holocene transgression (Troiani et al. 2011; Paine and Morton, 1993; Nelson and Bray, 1970). Presently, the Aransas River, the Mission River, and Copano Creek bring fresh water into Copano Bay while saltwater exchange occurs via the 2.5 km pass into Aransas Bay. Water temperatures in the bay can vary between 7 °C and 27 °C through the year (Calnan, 1980). Episodic tropical storms and hurricanes can produce storm surges that have the potential to shift sediment throughout the bay (Morton and McGowen, 1980).

The sediments in Copano Bay can be sorted into three distinct categories (Figure 1): muddy, sandy, and shelly (Calnan, 1980; Troiani et al, 2011). Dark-grey, homogenous, and structureless muddy sediments (10% very fine sand, 60% silt, 30% clay) that contain few shell fragments tend to be found in the deeper central bay. Lighter-grey homogenous and structureless sandy sediments (85% upper very fine sand, 15% silt) are found around the bay margins. Shelly sediments predominantly composed of large oyster fragments are associated with long and narrow oyster reefs throughout the bay interior.

Bioturbation in the muddy inner-bay sediments is dominated by a variety of small polychaetes, arthropods, and mollusks that are restricted to near-surface sediments (personal observation). In contrast, along the sandy bay margins, bioturbation is dominated by razor clams and thalassinid shrimp, which can burrow to a depth of at least 35 cm (Olszewski and Kaufman, 2015).

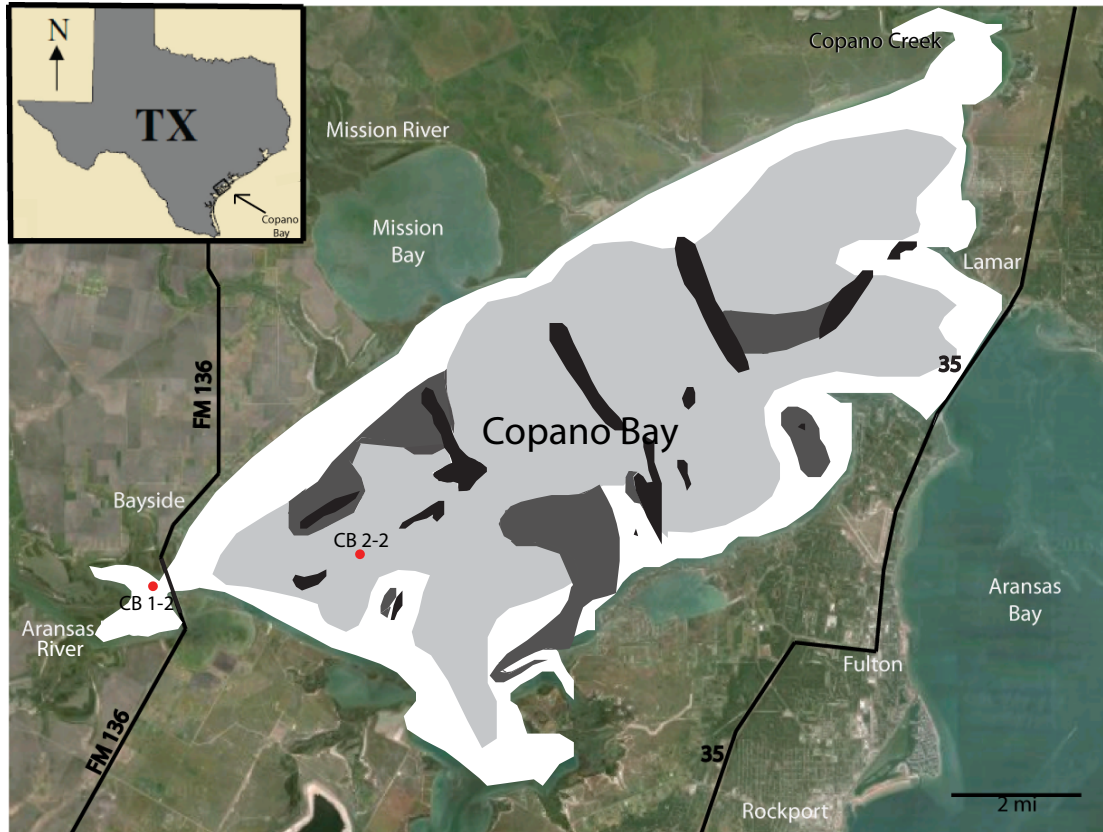


Figure 1: Location and facies map of Copano Bay, Texas (modified from Olszewski and Kaufman, 2015). White is sandy sediment, gray is muddy sediment, dark grey is shelly sediment, and black represents oyster reefs. Sites CB 1-2 (Delta Platform) and CB 2-2 (Estuary) are indicated.

3. SEDIMENTOLOGY

3.1 Methods

Sediment samples were obtained from 3-m-long, 3-in-diameter (7.5 cm) vibracores taken from the platform of the Aransas River delta (CB 1-2) and the open waters of Copano Bay (CB 2-2). The core sites correspond to the approximate locations of sampling sites C (platform) and A (estuary) from Olszewski and Kaufman (2015).

Sediment cores were split at the Texas A&M University-Galveston Sediment Laboratory. Both halves were photographed and described for sediment texture, grain-size distribution, color, and structure. X-rays were taken to help identify sedimentary structures.

Sediment samples for grain-size analysis were collected every 10 cm from both cores. Measurements were performed on a Malvern Mastersizer 3000 laser particle-size analyzer, which produces a grain-size distribution ranging from .01 μm to 3500 μm . The standard refractive index of 1.544 for quartz was used and each measurement was repeated 5 times to test for consistency (Miller and Schaetzl, 2011).

3.2 Results

3.2.1 Core Description

Sediment from both cores was examined with the unaided eye and using a 10x magnifier in order to describe fabric, physical sedimentary structures, and biogenic traces.

Core CB 1-2 (Figure 2) from the delta platform was composed of dark gray silty mud at the base that coarsened upward into a dark gray, subrounded, upper-fine grained sand. Core CB 2-2 from the estuary was composed of dark gray upper-fine grained sand at the base that fined upward into a dark gray clay mud. Both cores had shell concentration layers (SCLs) (Figure 2), i.e., visually identified layers that had an elevated abundance of shells compared to the surrounding sediment. Troiani et al. (2011) interpreted SCLs as storm deposits. SCLs were more common and uniformly distributed in core CB 2-2; only two SCLs were observed in the uppermost 250 cm in core CB 1-2. Core CB 1-2 had a burrow at a depth of 183 cm and core CB 2-2 did not have any shells in the uppermost 20 cm.

3.2.2 Grain Size

Thirty-seven grain size samples were collected from core CB 1-2 and twenty-eight from core CB 2-2. The sediments from core CB 1-2 exhibited a sharp change in grain size at ~275 cm from sand to silt (Figure 3). Above this horizon, median grain size coarsened upward from 10 μm to 85 μm and sorting improved from medium to well. The sediments from core CB 2-2 displayed an overall fining-upwards trend interrupted by two apparently coarse intervals that occurred at 80 and 60 cm depth. Samples from these

layers appear to have included shell fragments, whereas all other samples included only the sedimentary matrix.

The grain-size distributions through core CB 1-2 shift from skewed unimodal around 250-275 cm deep to bimodal between 170-0 cm deep. The grain-size distributions in core CB 2-2 were bimodal throughout the core, with a finer mode at ~ 4 μm and a coarser mode at ~ 100 μm . The finer mode is interpreted to represent fluvial suspended load, and the coarser mode, which is more prominent on the delta platform, is interpreted as fluvial bedload (Troiani et al., 2011).

3.2.3 Facies Analysis

Two sedimentary facies (Table 1) were identified in the cores from Copano Bay: *Mud* and *Sand*. These facies were characterized by different grain size, color, internal structure, and biotic content that represent different depositional conditions.

Mud Facies

Description

The Mud Facies is a well-sorted grey, homogenous, and structureless mud that contains sparse plant debris and does not have visible burrows. The alternations of SCLs and muddy layers, which are more easily seen in the x-radiographs than the photographs of the cores, do not demonstrate an obvious vertical trend in frequency or thickness. Sediment of the Mud Facies has a modal grain size ~ 4 μm .

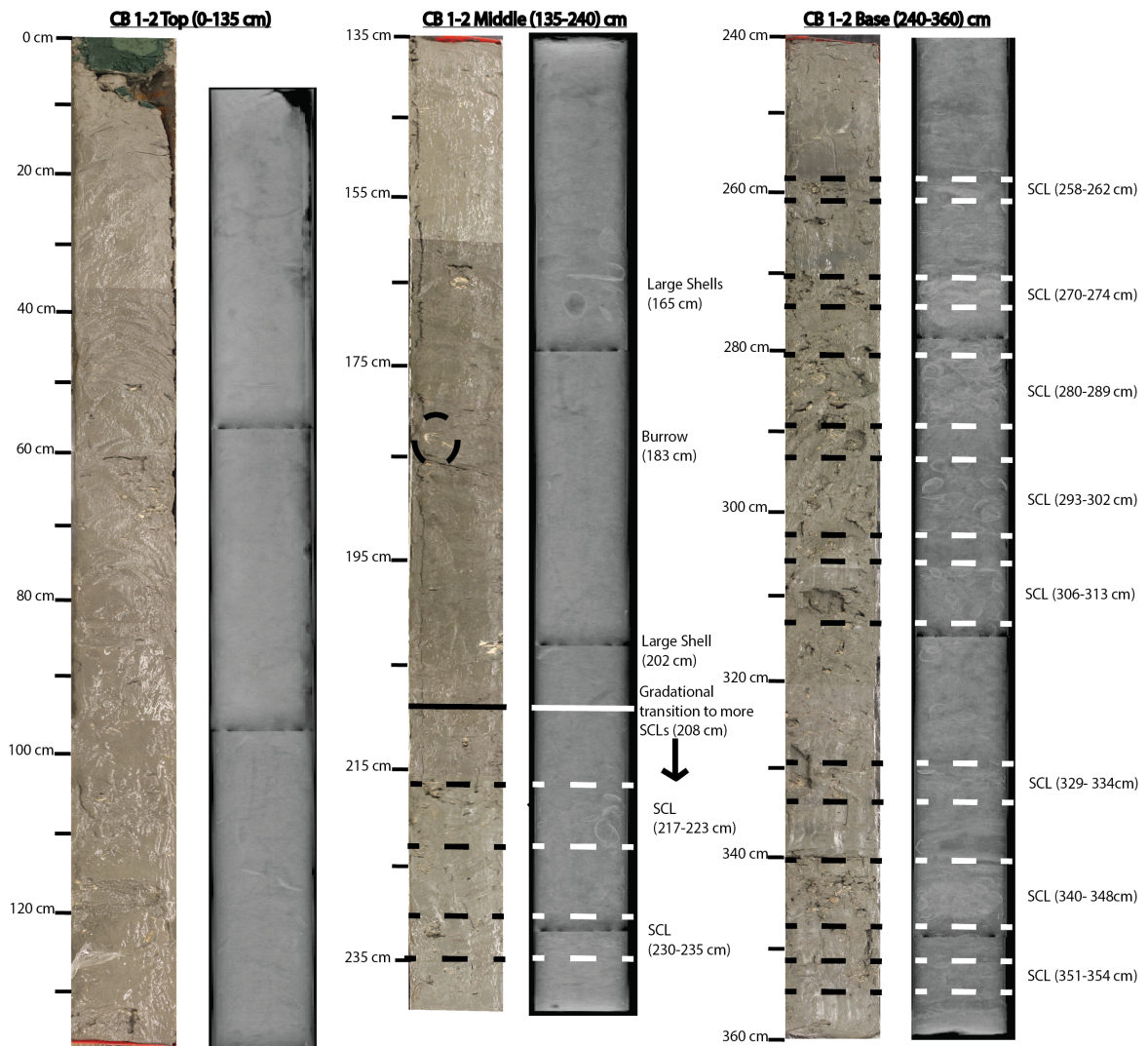


Figure 2: Sediment cores, measured sections, and x-rays of Core CB 1-2 (Top) and Core CB 2-2 (Bottom). The width of each core is 3 inches (7.5 cm).

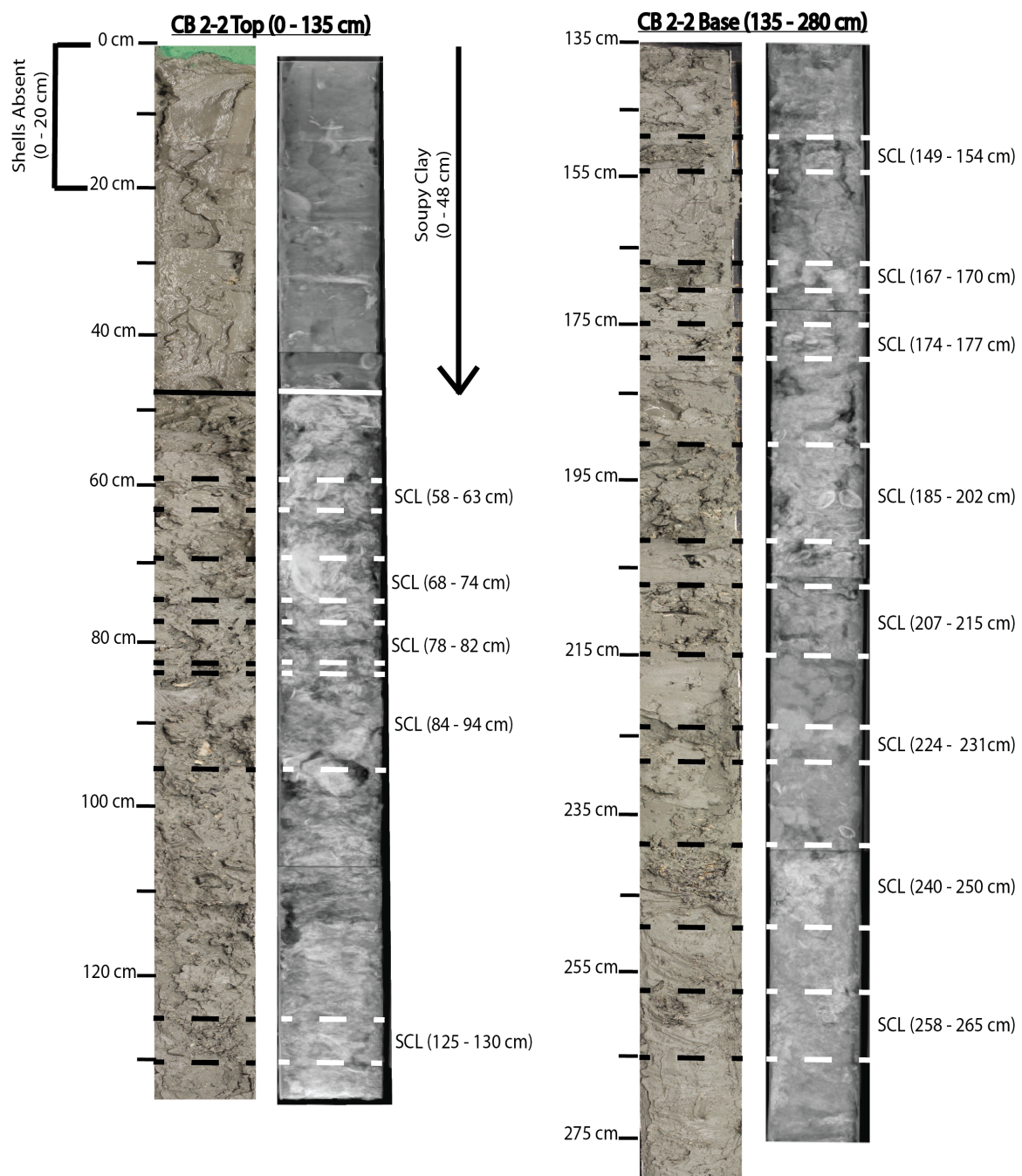


Figure 2: Continued.

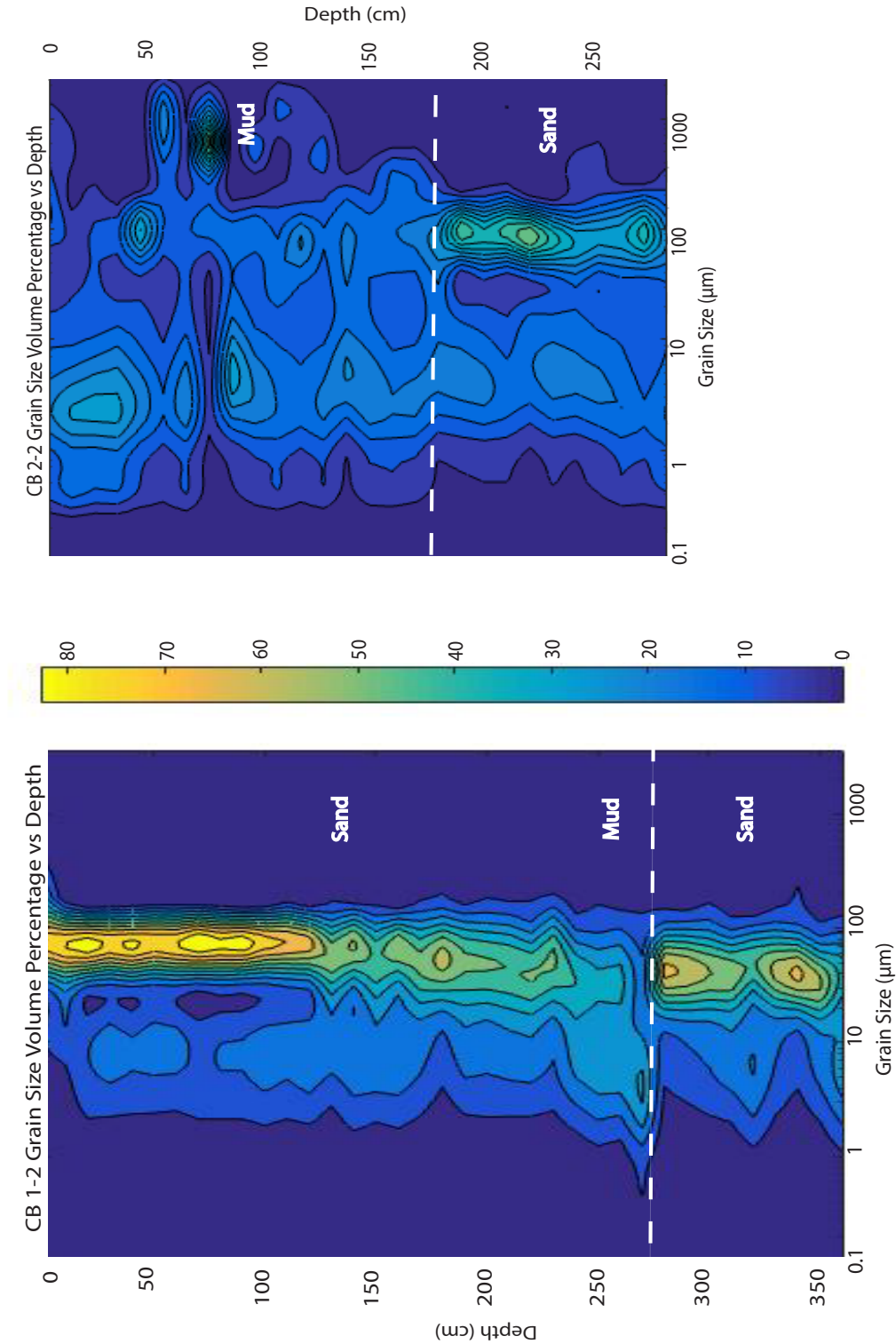


Figure 3: Grain size distribution vs. depth for each core site. The legend gives the percentage of grains at a given size per sample. The white dashed line represents a flooding surface.

Interpretation

The large percentage of mud (Table 1) and the lack of a sand component suggest that the Mud Facies represents a low-energy estuarine environment dominated by the settling of suspended material (Brown, 1989). The interbedded SCLs in the Mud Facies represent punctuated depositional events, likely associated with hurricanes and tropical storms that transport and concentrate coarser material.

Sand Facies

Description

The Sand Facies is a well-sorted homogenous and structureless sand that contains plant debris and shell fragments of *Chione elevata*, *Nuculana concentria*, *Rangia flexuosa*, and *Mulinia lateralis* uniformly distributed throughout. SCLs are sparse in the Sand Facies and burrows are present. The Sand Facies has a grain size mode at ~ 100 μm .

Interpretation

The Sand Facies represents a delta platform environment. SCLs are infrequent because post-depositional reworking from razor clams and thalassinid shrimp resulted in the homogenization of sediment (Matisoff, 1982; Cutler and Flessa, 1990; Kosnik et al., 2007).

Table 1: Sedimentary facies.

Facies	Description and features	Grain Size	Depositional Environment
Mud	Gray homogenous and structureless mud with sparse plant material, no burrows, and SCLs	10% fine sand, 60% silt, 30% clay	Estuary
Sand	Well-sorted homogenous and structureless sand with abundant plant debris and shell fragments, sparse burrows, and SCLs	85% upper very fine sand, 15% silt	Delta Platform

3.3 Depositional Model

The continuous vertical succession of sediment in CB 1-2 (Figure 3) shows a fining-upward succession consistent with a prograding delta. In core CB 1-2, the Mud Facies sharply overlies the Sand Facies at 275 cm below the sediment surface, indicating a flooding surface. Above the flooding surface, estuary deposits interbedded with SCLs gradationally coarsen upward into well-sorted delta platform deposits with sparse SCLs. In CB 2-2, a flooding surface occurs at a depth of ~175 cm in which the Mud Facies overlies the Sand Facies. The flooding surface in both cores is interpreted to correlate and may correspond to a seismic reflector identified by Troiani et al. (2011; their E5 surface) that those authors interpreted to have formed ~2500 years ago as a result of increased sediment flux entering Copano Bay.

4. SHELL AGE SPECTRA

4.1 Methods

4.1.1 Sampling

Mulinia lateralis is a small bivalve that has a broad geographic range extending from New Jersey to the Yucatan Peninsula (Winn and Knott, 1992). This species was chosen for age dating because: 1) it is large enough to produce the necessary amount of material needed for amino acid dating (adults are 10-15 mm in length, juveniles range from 200 to 700 μm), 2) it is abundant in surface and core sediments in Copano Bay, and 3) it burrows no deeper than a few centimeters below the sediment-water interface, so when it dies, it effectively begins its postmortem history at the surface.

Surface samples were acquired from the platform (CB 1-2) and estuary (CB 2-2) of the Aransas River bay-head delta by deploying a van Veen grab from a boat. These samples represent modern unconsolidated surface deposits that were collected to characterize the age distribution of shells being incorporated into the aggrading sediment column.

4.1.2 Amino Acid Racemization

Amino acids are chiral molecules – i.e., they have both a left-handed form and a right-handed form. All living organisms use amino acids only in the L-form; however, upon death, the L-amino acids racemize (i.e., spontaneously switch) to the D-form. The D/L ratio measures the extent of racemization. This ratio increases with time until the rate

of formation of D amino acids is compensated by the reverse reaction at which point racemic equilibrium is achieved (Mitterer, 1993; Goodfriend et al., 2000). Because the rate of racemization is influenced by extrinsic factors, it is necessary to calibrate D/L ratios using specimens whose age was determined independently. A number of previous studies (Wehmiller and Belknap, 1982; Wehmiller, 1993; Simonsen et al., 2013) have identified both physical and chemical sources of AAR.

First, intrashell variability (i.e., when different parts of the same shell are analyzed) can range as high as 10% depending on the species used for sampling (Carroll et al., 2013). In this study, whole specimens were analyzed when possible. However, in situations where this was not possible or the specimen was too big for AAR analysis, only the hinge was used because it is likely to be the oldest part of the shell (Goodfriend et al., 1997).

Second, different species can undergo racemization at different rates (Kidwell et al., 2005; Kosnik and Kaufman, 2008). For this reason, only *M. lateralis* was used.

And finally, temperature variations through time can bias D/L age estimates. For every 1°C increase in temperature, racemization will increase by ~20% (Williams and Smith, 1977). As a result, diurnal and seasonal temperature extremes can impact samples collected in the top meter or so of the sediment column.

4.1.3 Amino Acid Analyses

This study used liquid chromatographic resolution to determine the D/L ratios of aspartic (Asp) and glutamic (Glu) acids. 60 surface specimens from both sites as well as 293 specimens from core CB 1-2 and 209 specimens from core CB 2-2 were

analyzed at the Northern Arizona University Amino Acid Geochronology Laboratory. Shells were cleaned by ultrasonication in water for 1-minute increments until the bath water was clear; they were then leached with 2M HCL to remove 33% of the shell's outer mass. The larger shells were split and subsampled with a portion retained for analysis by AMS ^{14}C while the smaller shells were analyzed entirely. Each shell was left to dry under laminar flow and then hydrolyzed separately by being dissolved in 6M HCL. To recover the total hydrolyzable amino acid population while minimizing induced racemization (Kaufman and Manley, 1998), the solutions were heated for 6 hours at 110°C under N₂. The hydrolysates were evaporated to dryness *in vacuo*, then rehydrated with 0.01 M L-*homo*Arganine (L-hArg) to quantify the abundance of amino acids. Finally, serine was used to screen for possible secondary contamination prior to calibration (Kosnik et al., 2008).

4.1.4 Age Model

In order to calibrate D/L ratios to time, nine shells from the two cores were selected for analysis by AMS ^{14}C . These shells were uniformly selected between the highest and lowest D/L values measured (Figure 4) (Kosnik et al., 2008).

Because atmospheric carbon can reside in the ocean for tens to thousands of years before it is incorporated into living tissue, the apparent radiocarbon ages of marine samples are generally much older than their true ages (Stuiver and Braziunas, 1993). To correct for this marine reservoir effect, the nine shells that were dated by AMS ^{14}C were calibrated to calendar years using the MARINE13 curve in CALIB 7.1 with $\Delta\text{R} = -30 \pm 9$ years and a marine reservoir age of 439 ± 9 years (Wagner et al., 2009).

Numerical ages of both Asp and Glu were obtained by regressing the calibrated ^{14}C dates against the D/L values using the nine specimens collected from CB 1-2 and CB 2-2 plus ten live-collected and four core specimens (collected at the same location as CB 1-2) used previously by Olszewski and Kaufman (2015). Despite multiple efforts, no live specimens were collected at either site, suggesting that live populations of *Mulinia lateralis* were not present at the time of sampling. Instead, ten live specimens from throughout Copano Bay (Olszewski and Kaufman, 2015) were used to constrain the degree of amino acid racemization in living specimens (i.e., postmortem age of 0 years). A function of the form $t = m(\text{D/L})^x + b$ was used to best fit the Asp and Glu data (Figure 5), in which m = effective racemization constant (yr), t = estimated shell age (yr), b = predicted age when $\text{D/L} = 0$ (yr), and x = an exponent that best linearizes the relationship between time and D/L (Kosnik et al., 2008; Olszewski and Kaufman, 2015). This was done in MATLAB using the curve fitting toolbox.

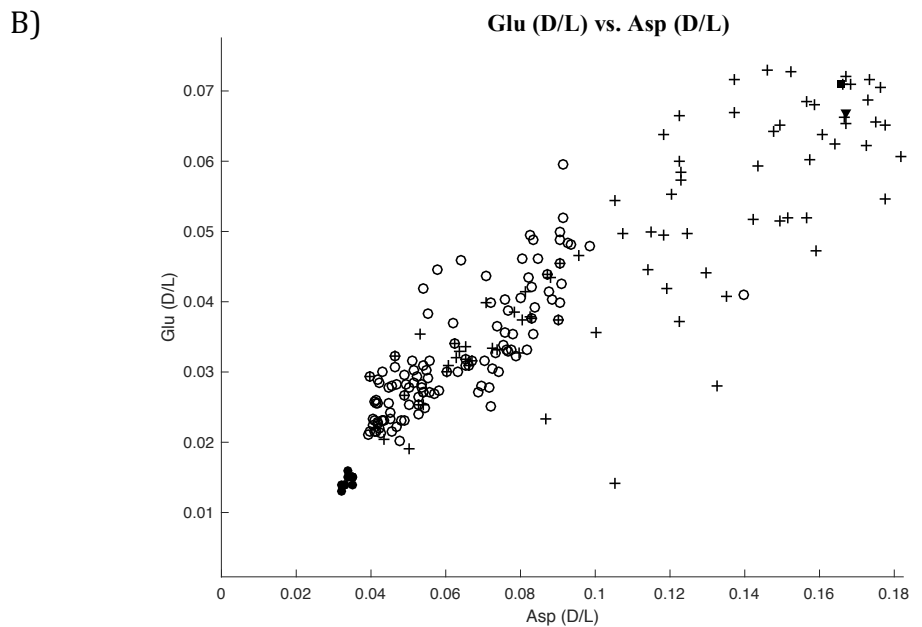
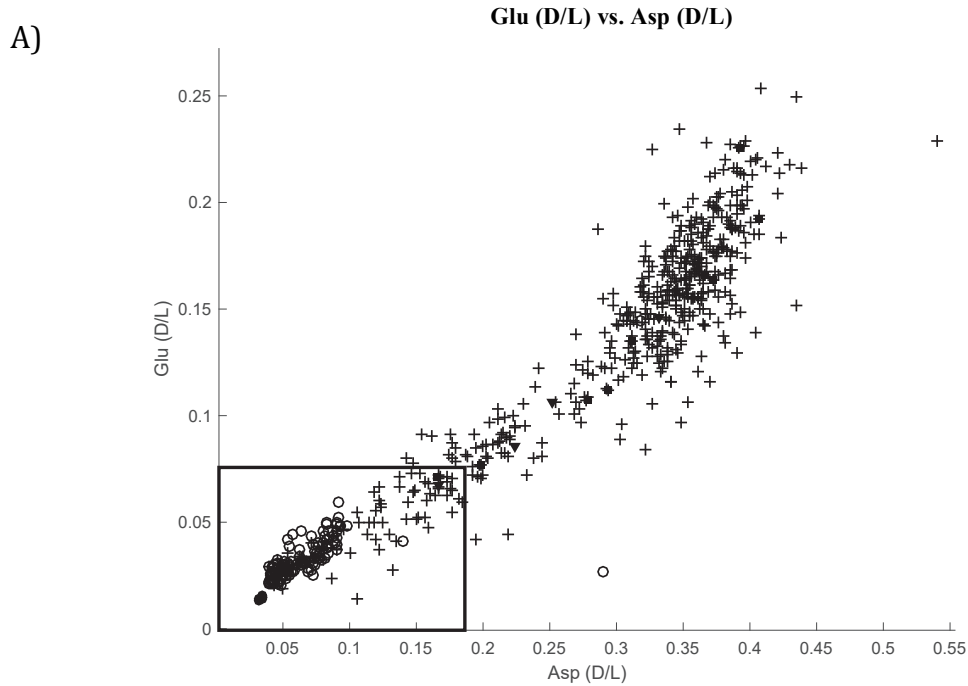


Figure 4: Glutamic and Aspartic amino acid D/L ratios. Crosses represent specimens from core samples, circles represent specimens from surface samples, filled circles are live-collected specimens, filled squares are radiocarbon-dated core specimens from this study, and filled triangles are radiocarbon-dated specimens from Olszewski and Kaufman (2015). **A)** All specimens. **B)** Inset square indicated in top view.

Because ^{14}C calibration curves can have uncertainties associated with their final calendar ages (Kosnik et al., 2008), several alternatives that weighted live-collected and postmortem specimens differently were tried to test for the most consistent D/L and ^{14}C age relationship for Asp- and Glu-based estimates. Following Kosnik et al. (2008), major-axis regressions in which live-collected specimens were treated as individual data points (all live-collected and ^{14}C -dated specimens weighted equally) were compared to major-axis regressions in which the intercepts were fixed at the mean D/L value of live-collected specimens (the live-collected specimens carry more weight). The regressions in which all ^{14}C and live-collected specimens were given equal weights produced the most consistent Asp and Glu age models (Table 2). The intercepts of both the Asp and Glu regressions were greater than 0 (0.9575 years and 44.56 years, respectively), resulting in inflated age estimates. To account for this effect, all age estimates had the regression intercept ages subtracted.

In order to detect age outliers for all specimens, a major-axis regression of Asp-age vs. Glu-age was carried out (Bevington and Robinson, 2003). However, the core specimens displayed a substantially different trend than the surface specimens. As a result, major-axis regressions were applied to both the core and surface specimens separately (Figure 6, Table 2). Surface or core specimens with Asp- or Glu- age values that fell beyond $\pm 2\sigma$ of the trend for their respective group were rejected.

The slope of the major axis regression of Asp- vs Glu- ages for specimens from the cores was significantly greater than 1 (Table 2), indicating that Glu ages consistently increased at a faster rate than Asp ages, however the Glu ages offered unrealistic surface values. For this reason, only Asp-based age estimates were used from this point forward.

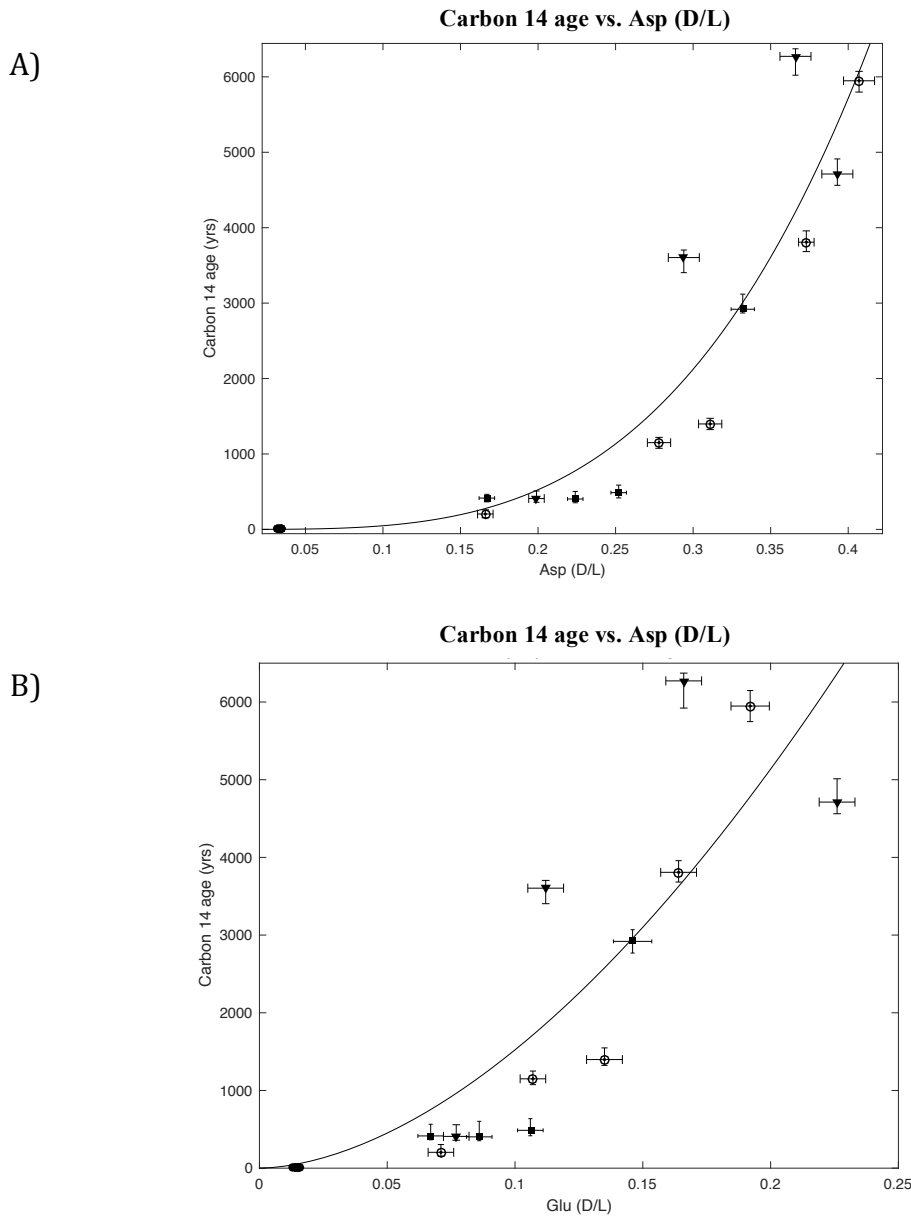


Figure 5: Amino acid age models. **A)** Aspartic acid. **B)** Glutamic acid. I-bars represent 95% confidence intervals around radiometric age estimates and Asp D/L and Glu D/L values. Model function: $t = m(D/L)^x + b$. Aspartic acid parameters (and standard error): $m = 1.34 \times 10^5$ (8.367×10^4), $b = 0.9575$ (0.039), $x = 3.443$ (0.626). Glutamic acid parameters (and standard error): $m = 8.643 \times 10^4$ (5.905×10^3), $b = 44.56$ (6.55), $x = 1.754$ (0.388). Filled circles are live-collected specimens, filled squares are specimens from Olszewski and Kaufman (2015), filled triangles are specimens from CB 1-2, and open circles are specimens from CB 2-2.

Table 2: Major-axis regression of Glu-based versus Asp-based age estimates.

	r (p)	slope (95% CI)	Intercept (95% CI)
Calibration specimens (' ¹⁴ C-dated + live)	0.965 (4.216 X 10 ⁻²⁰)	0.833 (0.761 to 0.904)	45.2 (29.8 to 60.9)
Core + surface specimens	0.724 (1.544 X 10 ⁻⁴³)	1.199 (1.055 to 1.344)	56.7 (40.1 to 73.3)
Core Specimens	0.778 (1.779 X 10 ⁻⁶⁹)	1.436 (1.339 to 1.534)	25.5 (8.3 to 42.7)
Surface Specimens	0.694 (7.740 X 10 ⁻⁴⁰)	1.092 (0.992 to 1.192)	60.5 (45.3 to 75.7)

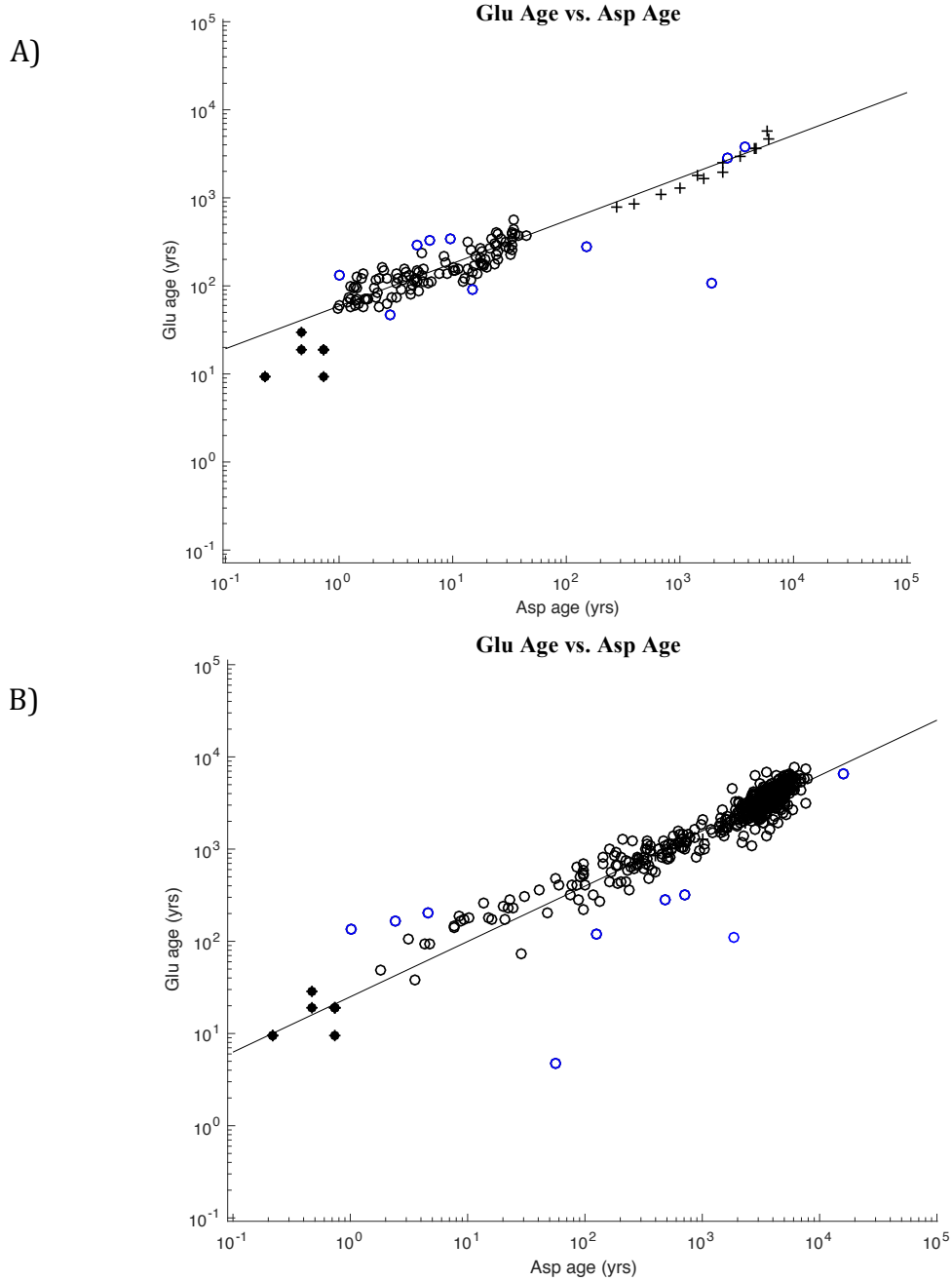


Figure 6: Scatterplot of Glu-based and Asp-based age values. **A)** Surface Specimens. **B)** Core Specimens. Filled circles represent specimens collected alive and crosses are radiocarbon-dated specimens, AAR age estimates of these shells are included solely for reference. Solid line is a major-axis regression based on \log_{10} -transformed **(A)** surface specimen age estimates (slope = 0.485; intercept = 60.012) and **(B)** core specimen age estimates (slope = 0.586; intercept = 25.001). Blue points indicate outliers.

4.2 Results

4.2.1 Shell Reliability

Generally, age estimates of shells are expected to increase with depth, however if shells achieve racemic equilibrium, their D/L ratio does not increase consistently over time and they no longer exhibit an age-depth relationship. In core CB 1-2, shells younger than ~1500 years yield a poor relationship between age and depth (Kendall's $\tau=0.3123$, $p\text{-value}=0.4532$; $R^2=0.1864$, $p\text{-value}=0.3121$), whereas in core CB 2-2 shells younger than ~1500 years produce a better relationship between age and depth (Kendall's $\tau=0.5899$, $p\text{-value}=1.0405 \times 10^{-7}$; $R^2=0.5963$, $p\text{-value}=2.0314 \times 10^{-10}$) (Figure 7). However, in both cores, shells older than ~1500 years do not exhibit an age-depth relationship. The lack of an age-depth relationship beyond ~1500 years suggests that shells in this study reached their racemic limit and any Asp-based estimates greater than ~1500 years are unreliable.

4.2.2 Shell Ages in the Sediment Column

To quantify the degree of mixing, the standard deviation of shell ages in each 10 cm sampling interval was calculated (Table 3). The results indicate a clear change in the range of ages from above 20 cm in CB 1-2 to below this depth in the core. Deeper than 20 cm, the standard deviation of ages within each bin was between 39.53 and 537.83 years with a mean value of 257.95 years.

In comparison, the standard deviation of postmortem ages in CB 2-2 is between 135.27 and 358.07 years with a mean value of 219.06 years. Unlike CB 1-2, the standard deviation increases with depth (Kendall's $\tau=0.768$, $p\text{-value}=1.03 \times 10^{-8}$).

Alternatively, shell age ranges can be calculated by subtracting the youngest shell from the oldest shell within each 10 cm sample interval (Figure 8, Table 3). In the samples from the uppermost 20 cm of CB 1-2, shell age ranges are between 8.44 and 69.66 years, whereas below 20 cm, age ranges are between 78.37 and 1031.69 years. These age ranges represent the scale of time averaging throughout most of core CB 1-2. Although the median ages of dated sampling intervals do not show a significant trend with depth (Kendall's $\tau= 0.136$, p -value=0.7572), these results demonstrate that the extent of time averaging increase dramatically below 20 cm.

In CB 2-2, no shells are present in the uppermost 20 cm of the core, but age ranges below 20 cm are between 393.92 and 743.89 years. Unlike CB 1-2, the median age of dated sampling intervals in CB 2-2 increases with depth (Kendall's $\tau= 0.678$, p -value= 1.15×10^{-8}).

A simple linear regression of age and depth (Figure 7) from each data set was used to estimate the sedimentation rate from each facies. The Sand Facies, from CB 1-2, yielded a sedimentation rate of 0.73 mm/yr (95% confidence bounds: 0.41, 1.05). The Mud Facies, from CB 2-2, produced a sedimentation rate of 0.29 mm/yr (95% confidence: 0.20, 0.38).

4.2.3 Postmortem Age Spectra in Surface Samples

The 56 dead shells from the sediment surface at site CB 1-2 range in age from 2.037 years to 34.288 years. Most of the shells are 2-3 years in age with a median of 2.62 years (Figure 9). The distribution is right-skewed and unimodal.

In comparison, the 56 dead shells from surface site CB 2-2 range in age from 2.86 years to 45.15 years. Most of the shells are ~20 years in age with a median of 18.11

years (Figure 9). Surface site CB 2-2 differs significantly from surface site CB 1-2 in terms of both median age and overall age distribution (Kolmogorov-Smirnov test statistic = .0333). Unlike surface site CB 1-2, which is right-skewed, surface site CB 2-2 is characterized by an age distribution that is much more uniform.

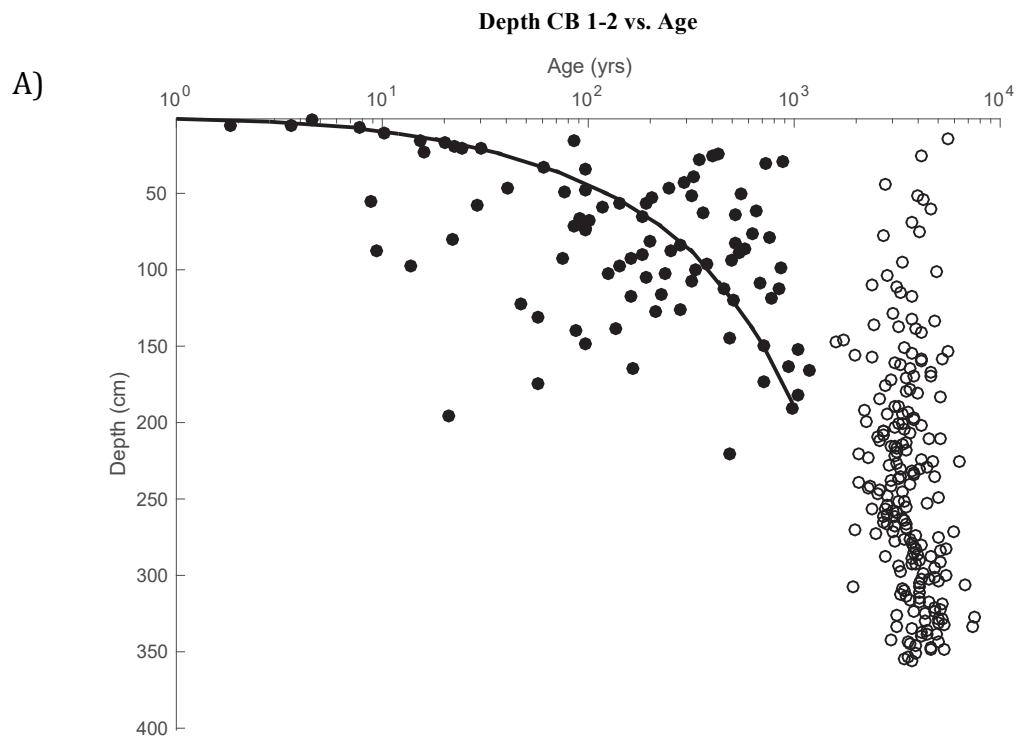


Figure 7: Depth vs. postmortem age plots. Note that the x-axis is logarithmic. Filled dots are reliable core specimens and unfilled circles are unreliable core specimens. Black regression lines are based only on reliable core specimens from both sites and were of the form $y=(m*x)$. Both regressions were fixed at an expected surface age of 0 to best fit the data. A) CB 1-2: $m= 0.07317$ (95% confidence: 0.04115, 0.1052) and B) CB 2-2: $m= 0.02898$ (95% confidence: 0.02039, 0.03756).

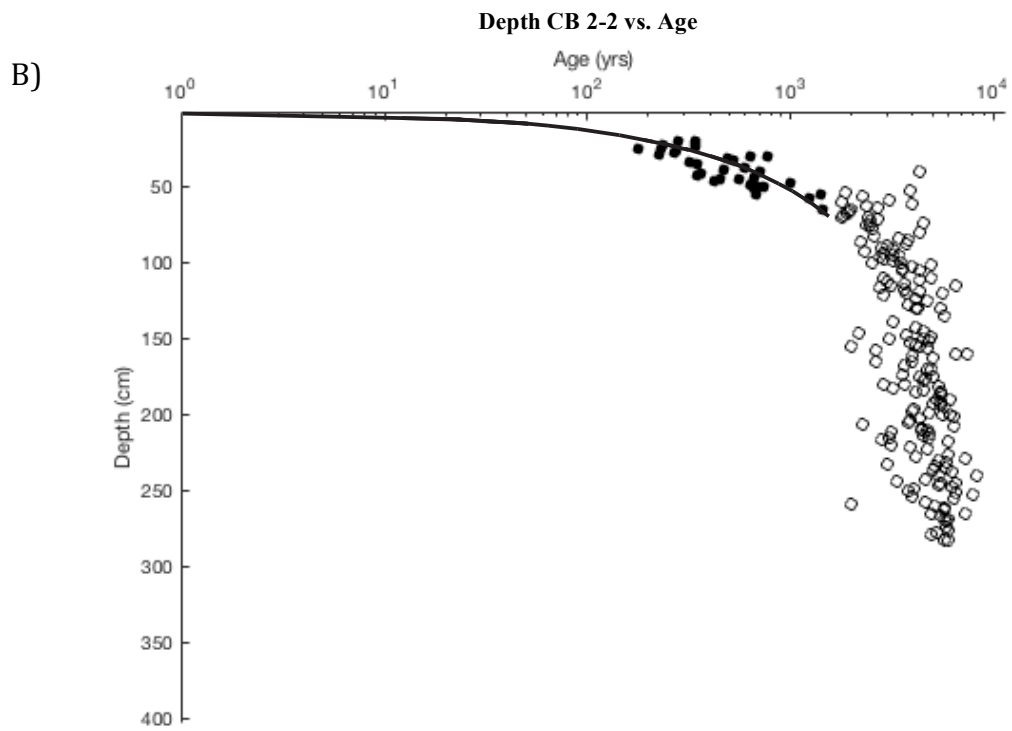


Figure 7: Continued.

Table 3: Summary of AAR chronology by sampled layers.

CB 1-2

Sample		AAR Shell Age (yrs)			Degree of Mixing		Age
Interval (cm)	n	min	med	max	Standard Deviation (yrs)	Range (yrs)	
1-10	6	1.82	4.70	10.26	3.04	8.44	
11-20	5	15.13	22.60	84.79	28.95	69.66	
21-30	6	15.86	373.86	886.12	319.48	870.26	
31-40	4	60.64	211.49	729.68	307.48	669.04	
41-50	6	40.55	171.90	550.67	191.18	510.12	
51-60	7	8.79	142.27	319.48	107.17	310.56	
61-70	6	90.21	271.53	652.02	233.17	561.81	
71-80	6	21.91	96.62	760.48	323.65	738.57	
81-90	8	9.30	267.90	572.90	203.14	563.6	
91-100	8	13.83	246.06	865.76	278.69	851.93	
101-110	5	126.26	238.43	687.81	221.06	561.55	
111-120	6	161.49	484.64	849.44	278.18	687.95	
121-130	3	47.52	211.63	278.41	118.82	230.89	
131-140	3	56.93	87.08	135.30	39.53	78.37	
141-150	3	96.14	482.13	706.77	308.84	610.63	
151-160	1	-	1038.06	-	-	-	
161-170	3	165.85	945.31	1197.54	537.83	1031.69	
171-180	2	56.60	389.72	716.84	466.86	660.24	
181-190	1	-	1040.50	-	-	-	
191-200	2	21.10	499.15	977.21	676.10	956.11	
221-230	1	-	481.24	-	-	-	

CB 2-2

Sample		AAR Shell Age (yrs)			Degree of Mixing		Age
Interval (cm)	n	min	med	max	Standard Deviation (yrs)	Range (yrs)	
11-20	1	-	337.82	-	-	-	
21-30	10	176.52	271.06	775.22	169.53	598.7	
31-40	8	317.77	506.27	711.69	135.27	393.92	
41-50	9	344.09	552.50	1008.90	213.36	664.81	
51-60	5	662.04	690.06	1405.93	358.07	743.89	
61-70	1	-	1455.89	-	-	-	
131-140	1	-	1449.13	-	-	-	

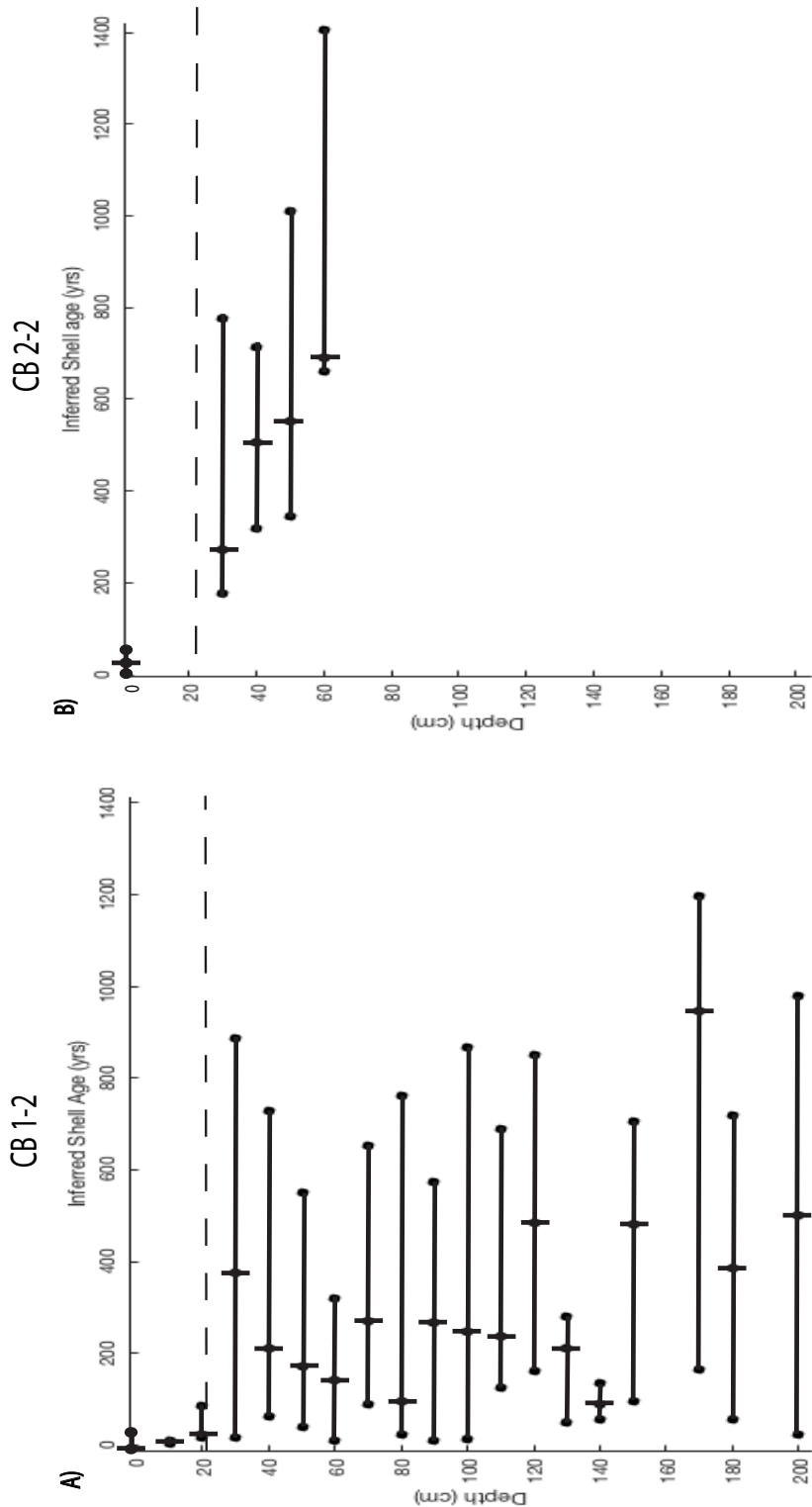


Figure 8: Inferred shell ages with sediment depth for both CB 1-2 (A) and CB 2-2 (B). The x-axis is shell age (yrs) and the y-axis is depth (cm). Black dots indicate the minimum and maximum AAR inferred shell age for each layer. The vertical bar is the median layer age.

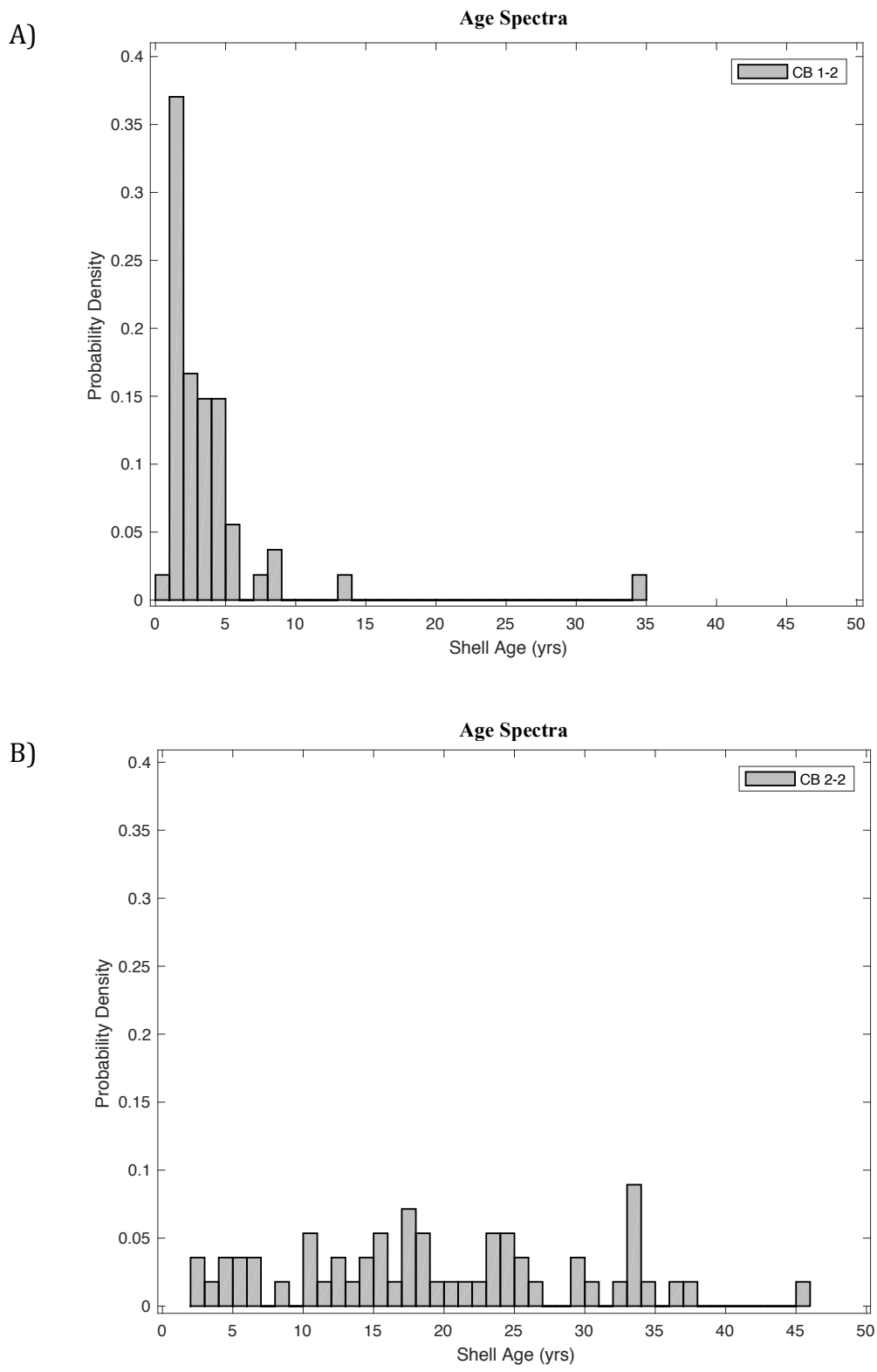


Figure 9: Surface age spectra for A) CB 1-2 and B) CB 2-2. Histogram bin size is 1 year.

5. DISCUSSION

Time averaging, the mixing of noncontemporaneous biologic material, is a ubiquitous property of fossil assemblages. Essentially, the scale of time averaging can be attributed to two factors: 1) stratigraphic condensation (governed by the rate of sediment accumulation)(Kidwell and Bosence, 1991; Mehldahl et al., 1997) and 2) reworking (governed by the rate of post-depositional mixing)(e.g., Kosnik et al., 2007, 2009, 2013; Tomasovich, 2014; Terry and Novak, 2015).

The rate of sediment accumulation determines the minimum possible degree of time averaging over a stratigraphic interval of given thickness (Meldahl et al., 1997).

Deposits formed under conditions of slow net sediment accumulation are more condensed and represent more time.

Sediment mixing, either physical or biogenic, causes further time averaging post-depositionally (Olszewski, 2004). The extent of time averaging is primarily governed by the rate and depth of mixing, with deeper and faster mixing leading to more time averaging (e.g., Olszewski, 2004; Kosnik et al., 2007, 2009, 2013; Tomasovich, 2014; Terry and Novak, 2015).

The distribution of postmortem ages of shells in a time-averaged accumulation reflects a balance between the influx of dead shells, the age of recycled dead shells incorporated into the deposit, the rate of destructive loss of shells, the rate and variability of sediment accumulation, and the nature and rate of sediment reworking (Olszewski, 2004; Olszewski and Kaufman, 2015). Although the right-skewed surface distribution from CB 1-2 (the delta platform) is consistent with rapid destruction of shells that are

being added to the sediment at an approximately constant rate, the overlap observed with the subsurface samples (Figure 8) indicates that surface shells are actively being incorporated into the aggrading sediment column. In contrast, the disconnect between the surface and subsurface spectra from CB 2-2 (the estuary) suggests that the two populations are isolated from one another (Olszewski, 2004).

Since surface shells from CB 1-2 are destroyed rapidly, these shells must also be rapidly introduced into the subsurface in order to be preserved. Shells can either enter the subsurface via burial at the surface, in which case they are expected to be close to their expected stratigraphic age, or through the deep burrows of razor clams and thalassinid shrimp (Aller, 1982), in which case they will be deeper than expected based on their age. Below 20 cm, the prominent increase in median shell age (Figure 8, Table 3) indicates that shells are relatively safe from destructive processes, however once shells enter the sediment column, they are then subject to additional mixing and stratigraphic disordering from bioturbation (Matisoff, 1982).

In contrast, the surface shells in CB 2-2 are isolated from subsurface shells. Unlike the subsurface data from CB 1-2, shells in the sediment column at CB 2-2 maintain their stratigraphic order. However, shells are completely absent from the uppermost 20 cm of sediment and there are no shells younger than 176.52 years in the subsurface. Without sediment mixing, each 10 cm sampling interval in the estuary is capable of preserving fossil assemblages with a temporal resolution of ~88 years (Kosnik et al., 2015), but the age ranges below 20 cm are 393.92 to 743.89 years (Table 3). This suggests mixing ~45 to 85 cm thick in the sediment column of the estuary.

The rate and depth of bioturbation relative to the net rate of sedimentation appears to be the primary constraint on time averaging in the vertical successions of the Aransas River delta. Without sediment mixing, each 10 cm sampling interval in CB 1-2 is capable of preserving fossil assemblages with a temporal resolution of ~35 years. However, the age ranges below 20 cm in CB 1-2 are 78.37 to 1031.69 years, suggesting mixing ~22.5 to 295 cm thick in the sediment column of the delta platform. As the Aransas River delta progrades, effective bioturbation (i.e., when the rate of reworking from bioturbation outweighs the net rate of sedimentation) vertically mixes shells from previously deposited estuary deposits. Such mixing results in stratigraphic disorder and subsurface postmortem shell age ranges that span the entire duration of deposition of the parasequence itself.

6. CONCLUSIONS

1. The net sediment accumulation rates of CB 1-2 and CB 2-2 are 0.73 mm/yr and 0.29 mm/yr, respectively. Based on the average sedimentation rate, each 10 cm sampling interval in CB 1-2, the delta platform, is capable of preserving fossil assemblages with a temporal resolution of ~35 years, however observed age ranges at depth (20 to 225 cm) are ~2.25 to 29.5x larger. In contrast, each 10 cm sampling interval in CB 2-2, the estuary, is capable of preserving fossil assemblages with a temporal resolution of ~88 years, however observed age ranges at depth (20 to 70 cm) are ~4.5 to 8.5x larger. These results imply that the rate and depth of reworking governs the magnitude of time averaging to a much larger degree than condensation in this depositional system.

2. Estuary sediment preserves a relatively more stratigraphically ordered deposit than the delta platform. However, in a prograding depositional system, such as the Aransas River delta, effective bioturbation can vertically rework previously deposited sediment. Such reworking can result in complete microstratigraphic disordering and time averaging that spans the entire duration of deposition of the progradational system, implying that shells found within several centimeters of each other in a parasequence reflect time averaging at the scale over which the progradational system itself evolves.

REFERENCES

- Aller, R.C. (1982) Carbonate dissolution in nearshore terrigenous muds: the role of physical and biological reworking: *Journal of Geology*, v. 90, p. 79–95
- Behre, K.E. (2004) Coastal development, sea-level change and settlement history during the later Holocene in the Clay District of Lower Saxony (Niedersachsen), northern Germany: *Quatern Int*, v. 112, p. 37-53
- Bevington, P.R. and Robinson, D.K. (2003) Data Reduction and Error Analysis for the Physical Sciences, Third Edition, *McGraw-Hill, Inc.*, New York.
- Brown, J. (1989) Waves, tides and shallow-water processes: *Oxford University Press*, p. 187
- Bungenstock, F. and Schäfer, A. (2009) The Holocene relative sea-level curve for the tidal basin of the barrier island Langeoog, German Bight, Southern North Sea: *Global and Planetary Change*, v. 66, p. 34-51
- Calnan, T.R. (1980) Molluscan Distribution in Copano Bay, Texas: *Texas Bureau of Economic Geology Report of Investigations*, v. 103, p. 71
- Carroll, M., Kowalewski, M., Simões, M.G., and Goodfriend, G.A. (2003) Quantitative estimates of time-averaging in terebratulid brachiopod shell accumulations from a modern tropical shelf: *Paleobiology*, v. 29, p. 381–402
- Chang, T.S., Flemming, B.W., Tilch, E., Bartholoma, A., and Wostmann, R. (2006) Late Holocene stratigraphic evolution of a back-barrier tidal basin in the east Frisian Wadden Sea, southern North Sea: Transgressive Deposition and its Preservation Potential: *Facies*, v. 52, p. 329-340
- Cubizolle, H., Bonnel, P., Oberlin, C., Tourman, A., and Porteret, J. (2007) Advantages and limits of radiocarbon dating applied to peat inception during the end of the late glacial and the Holocene: the example of mires in the eastern Massif Central (France): *Quaternary Reviews*, v. 18, p. 187-208
- Davis, R.A., Bartholdy, J., and Lykke-Andersen, H. (2001) Sedimentary depositional environments and Holocene geologic evolution of the northern Danish Wadden Sea: *Korean Society of Oceanography, Special Publication, Proceedings of Tidalite 2000*, p. 63-75
- Denys, L. and Baeteman, C. (1995) Holocene evolution of relative sea-level and local mean high water spring tides in Belgium – A First Assessment: *Mar Geol*, v. 124, p. 1-19

- Dexter, T.A., Kaufman, D.S., Kruase, R.A., Jr., Barbour Wood, S.L., Simões, M.G., Huntley, J.W., Yanes, Y., Romanek, C.S., and Kowalewski, M. (2014) A continuous multi-millennial record of surficial bivalve mollusk shells from the São Paulo Bight, Brazilian shelf: *Quaternary Research*, v. 81, p. 274–283
- Flessa, K.W. (1993) Time-averaging and temporal resolution in recent shelly faunas, in Kidwell, S.M., and Behrensmeyer, A.K., eds., *Taphonomic Approaches to Time Resolution in Fossil Assemblages*, Short Courses in Paleontology No. 6: Knoxville, Tennessee: *Paleontological Society*, p. 9–33
- Flessa, K.W., and Kowalewski, M. (1994) Shell survival and time-averaging in nearshore and shelf environments: estimates from the radiocarbon literature: *Lethaia*, v. 27, p. 153–165
- Goodfriend, G.A., Flessa, K., Hare, P. (1997) Variation in amino acid epimerization rates and amino acid composition among shell layers in the bivalve *Chione* from the Gulf of California: *Geochimica et Cosmochimica Acta*, v. 61, p. 1487-1493
- Goodfriend, G.A., Collins, M.J., Fogel, M.L., Macko, S.A., and Wehmiller, J.F. (2000) Perspectives in Amino Acid and Protein Geochemistry: New York, *Oxford University Press*, p. 366
- Heron, S.D., Moslow, T.F., Berelson, W.M., Herbert, J.R., Steele, G.A., and Susman, K.R. (1984) Holocene sedimentation of a wave-dominated barrier-island shoreline – Cape Lookout, North-Carolina: *Mar Geol*, v. 60, p. 413-434
- Kaufman, D.S., and Manley, W.F. (1998) A new procedure for determining D/L amino acid ratios in fossils using reverse phase liquid chromatography: *Quaternary Science Reviews*, v. 17, p. 987-1000
- Kidwell, S. M., and D.W. J. Bosence. (1991) Taphonomy and time averaging of marine shelly faunas. In P. A. Allison, and D. E. G. Briggs, eds. *Taphonomy: releasing data locked in the fossil record*: *Topics in Geobiology* 9, Plenum Press, New York, p. 115–209
- Kidwell, S.M., Best, M.M.R., and Kaufman, D.S. (2005) Taphonomic trade-offs in tropical marine death assemblages: differential time averaging, shell loss, and probably bias in siliciclastic vs. carbonate facies: *Geology*, v. 33, p. 729–732
- Kosnik, M.A., Hua, W., Jacobsen, G.E., Kaufman, D.S., and Wust, R.A. (2007) Sediment mixing and stratigraphic disorder revealed by the age-structure of *Tellina* shells in Great Barrier Reef sediment: *Geology*, v. 35, p. 811–814
- Kosnik, M.A., and Kaufman, D.S. (2008) Identifying outliers and assessing the accuracy of amino acid racemization measurements for geochronology: II. Data screening: *Quaternary Geochronology*, v. 3, p. 328–341

- Kosnik, M.A., Kaufman, D.S., and Hua, Q. (2008) Identifying outliers and assessing the accuracy of amino acid racemization measurements for geochronology: I. Age calibration curves: *Quaternary Geochronology*, v. 3, p. 308–327
- Kosnik, M.A., Hua, Q., Kaufman, D.S., and Wust, R.A. (2009) Taphonomic bias and time-averaging in tropical molluscan death assemblages: differential shell half-lives in Great Barrier Reef sediment: *Paleobiology*, v. 35, p. 565–586
- Kosnik, M.A., Hua, Q., Kaufman, D.S., and Zawadzki, A. (2015) Sediment accumulation, stratigraphic order, and the extend of time-averaging in lagoonal sediments: a comparison of ^{210}Pb and ^{14}C /amino acid racemization chronologies: *Coral Reefs*, v. 34, p. 215–229
- Kowalewski, M. (1996) Time-averaging, overcompleteness, and the geological record: *Journal of Geology*, v. 104, p. 317–326
- Kowalewski, M., Goodfriend, G.A., and Flessa, K.W. (1998) High-resolution estimates of temporal mixing within shell beds: the evils and virtues of time-averaging: *Paleobiology*, v. 24, p. 287–304
- Kraft, J.C., Chrzastowski, M.J., Belknap, D.F., Toscano, M.A., and Fletcher, C.H. (1987) The transgressive barrier-lagoon coast of Delaware: Morphostratigraphy, sedimentary sequences and responses to relative rise in sea level. In: *Sea-Level Fluctuation and Coastal Evolution* (Eds. Nummedal, D., Pilkey, O.H., and Howard, J.D.), p. 129–143. Society of Economic Paleontologists and Mineralogists, Tulsa
- Matisoff, G. (1982) Chapter 7. Mathematical models of bioturbation, in McCall, P.L., and Tevesz, M.J.S., eds.: *Animal-Sediment Relations: The Biogenic Alteration of Sediments*: New York, Plenum Press, p. 289–330
- McManus, J. (2002) Deltaic responses to changes in river regimes: *Marine Chemistry* 79, 155–170
- Meldahl K.H., Flessa K.W., Cutler A.H. (1997) Time-averaging and postmortem skeletal survival in benthic fossil assemblages: quantitative comparisons among Holocene environments: *Paleobiology*, v. 23, p. 207–229
- Miller, B.A., and Schaetzl, R.J. (2011) Precision of Soil Particle Size Analysis using Laser Diffractometry: *Soil Science Society of America Journal*, v. 76, p. 1719–1727
- Mitterer, R.M., (1993) The diagenesis of proteins and amino acids in fossil shells, in Engel, M.H., and Macko, S.A., eds.: *Organic Geochemistry*. New York, Plenum Press, p. 739–753

- Morton, R.A., and McGowen, J.H. (1980) Modern depositional environments of the Texas Coast, *Bureau of Economic Geology*, The University of Texas at Austin.
- Moslow, T.F. and Heron, S.D. (1979) Quaternary evolution of Core Banks, North Carolina: Cape Lookout to New Drum Inlet. In: *Barrier Islands – From the Gulf of St. Lawrence to the Gulf of Mexico* (Ed. Leatherman, S.P.), New York, Academic Press, p. 211-236
- Nelson, H.F. and Bray, E.E. (1970) Stratigraphy and history of the Holocene sediments in the Sabine-High Island area, Gulf of Mexico, in Morgan, J.P., and Shaver, R.H., eds., Deltaic Sedimentation, Modern and Ancient: *Society of Economic Paleontologists and Mineralogists Special Publication*, v. 15, p. 48–77
- Nichols, M.M., Johnson, G.H., and Peebles, P.C. (1991) Modern sediments and facies model for a microtidal coastal-plain estuary, the James Estuary, Virginia: *J Sediment Petrol*, v. 61, p. 883-899
- Nilsson, C., Reidy, C.A., Dynesius, Revenga, C. (2005) Fragmentation and flow regulation of the world's large river systems: *Science*, v. 308, p. 405–408
- Olszewski T.D. (1999) Taking advantage of time-averaging: *Paleobiology*, v. 25, p. 226–238
- Olszewski, T.D. (2004) Modeling the influence of taphonomic destruction, reworking, and burial on time-averaging in fossil accumulations: *PALAIOS*, v. 19, p. 39–50
- Olszewski, T.D. (2012) Remembrance of things past: modeling the relationship between species' abundances in living communities and death assemblages: *Biology letters*, v. 8, no. 1, p. 131–134, doi: 10.1098/rsbl.2011.0337
- Olszewski, T.D. and Kaufman, D.S. (2015) Tracing burial history and sediment recycling in a shallow estuarine setting (Copano Bay, Texas) using postmortem ages of the bivalve *Mulinia lateralis*: *PALAIOS*, v. 30 (3), p. 224-237
- Paine, J.G., and Morton, R.A. (1993) Historical Shoreline Changes in Copano, Aransas, and Redfish Bays, Texas Gulf Coast: *Texas Bureau of Economic Geology Geological Circular* 93-1, p. 66
- Pont, D., Day, J.W., Hensel, P., Franquet, E., Torre, F., Rioual, P., Ibanez, C., Coulet, E. (2002) Response scenarios for the deltaic plain of the Rhone in the face of an accelerated rate of sea-level rise with special attention to Salicornia-type environments: *Estuaries*, v. 25, p. 337–358
- Powell, E.N., Stanton, R.J., Jr., Logan, A., and Craig, M.A. (1992) Preservation of Mollusca in Copano Bay, Texas. The long-term record: *Palaeogeography, Palaeoclimatology, and Palaeoecology*, v. 95, p. 209–228

- Simonson, A.E., Lockwood, R., and Wehmiller, J.F. (2013) Three approaches to radiocarbon calibration of amino acid racemization in *Mulinia lateralis* from the Holocene of the Chesapeake Bay, USA: *Quaternary Geochronology*, v. 16, p. 62–72
- Stuiver, M. and Braziunas, T.F. (1993) Modeling atmospheric ^{14}C influences and ^{14}C ages of marine samples to 10,000 BC: *Radiocarbon*, v. 35, p. 137-189
- Tessier, B., Billeaud, I., Sorrel, P., Delsinne, N., and Lesueur, P. (2012) Infilling stratigraphy of macrotidal tide-dominated estuaries. Controlling mechanisms: Sea-level fluctuations, bedrock morphology, sediment supply and climate changes (The examples of the Seine estuary and the Mont-Saint-Michel Bay, English Channel, NW France): *Sediment Geol*, v. 279, p. 62-73
- Terry, R.C., and Novak, M., (2015) Where does the time go?: Mixing and the depth-dependent distribution of fossil ages: *Geology*, v. 43, p. 487-490
- Thom, B.G. and Roy, P.S. (1985) relative sea levels and coastal sedimentation in Southeast Australia in the Holocene: *J Sediment Petrol*, v. 55, p. 257-264
- Tomasovich, A., Kidwell, S.M., Foygel Barber, R., and Kaufman, D.S. (2014) Longterm accumulation of carbonate shells reflects a 100-fold drop in loss rate: *Geology*, v. 42, p. 819–822
- Troiani, B.T., Simms, A.R., Dellapenna, T., Piper, E., and Yokoyama, Y. (2011) The importance of sea-level and climate change, including changing wind energy, on the evolution of a coastal estuary: Copano Bay, Texas: *Marine Geology*, v. 280, p. 1–19
- Wagner, A.J., Guilderson, T.P., Slowey, N.C., and Cole, J.E. (2009) Pre-bomb surface water radiocarbon of the Gulf of Mexico and Caribbean as recorded in hermatypic corals: *Radiocarbon*, v. 51, p. 947–954
- Wehmiller, J.F. (1993) Applications of organic geochemistry for Quaternary research: aminostratigraphy and aminochronology. In: Engel, M., Macko, S. (Eds.), *Organic Geochemistry: Plenum Publishing Company*, p. 755-783
- Wehmiller, J.F., Belknap, D.F. (1982) Amino acid age estimates, Quaternary Atlantic coastal plain: comparison with U-series dates, biostratigraphy, and paleomagnetic control: *Quaternary Research*, v. 18, p. 311-336.
- Williams, K.M. and Smith, G.G. (1977) A critical evaluation of the application of amino acid racemization to geochronology and geothermometry: *Origins of Life*, v. 8, p. 91-144

Winn, R., Knott, D. (1992) An evaluation of the survival of experimental populations exposed to hypoxia in the Savannah River estuary: *Marine Ecology Progress Series*, v. 88, p. 161-179

APPENDIX

Table 4: CB 1-2 grain size distributions vs. depth.

Size (μm)	0 cm volume %	10 cm volume %	20 cm volume %	30 cm volume %	40 cm volume %
0.01	0	0	0	0	0
0.0114	0	0	0	0	0
0.0129	0	0	0	0	0
0.0147	0	0	0	0	0
0.0167	0	0	0	0	0
0.0189	0	0	0	0	0
0.0215	0	0	0	0	0
0.0244	0	0	0	0	0
0.0278	0	0	0	0	0
0.0315	0	0	0	0	0
0.0358	0	0	0	0	0
0.0407	0	0	0	0	0
0.0463	0	0	0	0	0
0.0526	0	0	0	0	0
0.0597	0	0	0	0	0
0.0679	0	0	0	0	0
0.0771	0	0	0	0	0
0.0876	0	0	0	0	0
0.0995	0	0	0	0	0
0.113	0	0	0	0	0
0.128	0	0	0	0	0
0.146	0	0	0	0	0
0.166	0	0	0	0	0
0.188	0	0	0	0	0
0.214	0	0	0	0	0
0.243	0	0	0	0	0
0.276	0	0	0	0	0
0.314	0	0	0	0	0
0.357	0	0	0	0	0
0.405	0	0	0.08	0.05	0.05
0.46	0	0	0.12	0.1	0.1
0.523	0	0	0.17	0.14	0.14
0.594	0	0.07	0.2	0.17	0.17
0.675	0.01	0.08	0.22	0.19	0.19
0.767	0.03	0.09	0.23	0.2	0.19
0.872	0.03	0.09	0.23	0.2	0.2
0.991	0.03	0.09	0.23	0.2	0.2
1.13	0.04	0.09	0.25	0.21	0.21

Table 4: Continued.

1.28	0.04	0.1	0.28	0.24	0.24
1.45	0.07	0.12	0.33	0.28	0.28
1.65	0.09	0.14	0.39	0.34	0.33
1.88	0.12	0.17	0.48	0.42	0.41
2.13	0.14	0.21	0.58	0.52	0.5
2.42	0.17	0.25	0.69	0.64	0.61
2.75	0.2	0.29	0.81	0.77	0.72
3.12	0.23	0.34	0.93	0.92	0.85
3.55	0.27	0.39	1.06	1.07	0.98
4.03	0.3	0.44	1.17	1.23	1.12
4.58	0.33	0.49	1.28	1.39	1.25
5.21	0.37	0.54	1.38	1.55	1.38
5.92	0.41	0.6	1.46	1.69	1.5
6.72	0.46	0.67	1.52	1.82	1.6
7.64	0.52	0.76	1.57	1.93	1.68
8.68	0.59	0.87	1.61	2.03	1.74
9.86	0.67	1.01	1.62	2.09	1.78
11.2	0.74	1.16	1.61	2.12	1.78
12.7	0.79	1.32	1.56	2.1	1.73
14.5	0.8	1.47	1.47	2.02	1.63
16.4	0.78	1.6	1.32	1.87	1.47
18.7	0.72	1.69	1.12	1.66	1.26
21.2	0.63	1.75	0.9	1.4	1.03
24.1	0.56	1.81	0.7	1.13	0.83
27.4	0.56	1.9	0.59	0.92	0.72
31.1	0.69	2.08	0.66	0.85	0.78
35.3	1.03	2.42	1	1.01	1.1
40.1	1.61	2.98	1.66	1.47	1.73
45.6	2.46	3.77	2.68	2.28	2.69
51.8	3.53	4.77	4	3.4	3.93
58.9	4.72	5.87	5.49	4.73	5.32
66.9	5.9	6.94	6.93	6.08	6.68
76	6.91	7.79	8.1	7.23	7.77
86.4	7.59	8.24	8.74	7.94	8.39
98.1	7.85	8.18	8.71	8.05	8.39
111	7.67	7.56	7.97	7.5	7.73
127	7.11	6.45	6.6	6.34	6.5
144	6.28	5.02	4.85	4.77	4.9
163	5.32	3.5	3.07	3.08	3.22
186	4.37	2.1	1.36	1.57	1.73
211	3.53	1	0.04	0.08	0.26
240	2.84	0.09	0	0	0
272	2.31	0.02	0	0	0
310	1.89	0	0	0	0
352	1.56	0	0	0	0

Table 4: Continued.

400	1.28	0.02	0	0	0
454	1.02	0.05	0	0	0
516	0.78	0.08	0	0	0
586	0.56	0.1	0	0	0
666	0.32	0.11	0	0	0
756	0.15	0.1	0	0	0
859	0.03	0.08	0	0	0
976	0	0.05	0	0	0
1110	0	0.03	0	0	0
1260	0	0	0	0	0
1430	0	0	0	0	0
1630	0	0	0	0	0
1850	0	0	0	0	0
2100	0	0	0	0	0
2390	0	0	0	0	0
2710	0	0	0	0	0
3080	0	0	0	0	0
3500	0	0	0	0	0
Size (μm)	50 cm volume %	60 cm volume %	70 cm volume %	80 cm volume %	100 cm volume %
0.01	0	0	0	0	0
0.0114	0	0	0	0	0
0.0129	0	0	0	0	0
0.0147	0	0	0	0	0
0.0167	0	0	0	0	0
0.0189	0	0	0	0	0
0.0215	0	0	0	0	0
0.0244	0	0	0	0	0
0.0278	0	0	0	0	0
0.0315	0	0	0	0	0
0.0358	0	0	0	0	0
0.0407	0	0	0	0	0
0.0463	0	0	0	0	0
0.0526	0	0	0	0	0
0.0597	0	0	0	0	0
0.0679	0	0	0	0	0
0.0771	0	0	0	0	0
0.0876	0	0	0	0	0
0.0995	0	0	0	0	0
0.113	0	0	0	0	0
0.128	0	0	0	0	0
0.146	0	0	0	0	0
0.166	0	0	0	0	0
0.188	0	0	0	0	0

Table 4: Continued.

0.214	0	0	0	0	0
0.243	0	0	0	0	0
0.276	0	0	0	0	0
0.314	0	0	0	0	0
0.357	0	0	0	0	0
0.405	0	0	0.08	0.08	0.08
0.46	0.09	0.08	0.12	0.12	0.12
0.523	0.13	0.12	0.16	0.17	0.17
0.594	0.16	0.15	0.2	0.2	0.2
0.675	0.17	0.16	0.22	0.22	0.22
0.767	0.18	0.17	0.22	0.23	0.22
0.872	0.18	0.17	0.23	0.23	0.23
0.991	0.18	0.18	0.23	0.23	0.23
1.13	0.19	0.19	0.25	0.25	0.25
1.28	0.22	0.21	0.28	0.28	0.28
1.45	0.25	0.25	0.33	0.32	0.32
1.65	0.31	0.3	0.4	0.39	0.39
1.88	0.39	0.37	0.49	0.48	0.48
2.13	0.48	0.45	0.59	0.58	0.58
2.42	0.58	0.55	0.7	0.69	0.69
2.75	0.7	0.66	0.82	0.82	0.82
3.12	0.83	0.78	0.94	0.95	0.94
3.55	0.96	0.91	1.06	1.08	1.08
4.03	1.11	1.05	1.17	1.21	1.2
4.58	1.25	1.2	1.26	1.33	1.33
5.21	1.39	1.35	1.33	1.44	1.44
5.92	1.53	1.49	1.39	1.54	1.53
6.72	1.66	1.63	1.43	1.61	1.61
7.64	1.78	1.76	1.44	1.67	1.67
8.68	1.89	1.88	1.45	1.71	1.71
9.86	1.98	1.96	1.44	1.72	1.73
11.2	2.03	2.01	1.41	1.7	1.73
12.7	2.05	2	1.36	1.65	1.69
14.5	2	1.92	1.26	1.55	1.61
16.4	1.89	1.76	1.12	1.41	1.47
18.7	1.71	1.54	0.94	1.22	1.28
21.2	1.47	1.27	0.73	1	1.05
24.1	1.22	1.02	0.52	0.8	0.83
27.4	1.02	0.84	0.39	0.68	0.67
31.1	0.95	0.83	0.41	0.71	0.65
35.3	1.08	1.06	0.69	0.98	0.86
40.1	1.51	1.61	1.29	1.55	1.39
45.6	2.26	2.5	2.25	2.45	2.28
51.8	3.32	3.67	3.55	3.65	3.5
58.9	4.59	5.01	5.08	5.04	4.95

Table 4: Continued.

66.9	5.91	6.35	6.63	6.43	6.45
76	7.06	7.45	7.98	7.61	7.74
86.4	7.82	8.11	8.86	8.34	8.59
98.1	8.03	8.17	9.08	8.47	8.77
111	7.61	7.6	8.57	7.91	8.2
127	6.59	6.48	7.38	6.73	6.93
144	5.16	4.98	5.72	5.13	5.18
163	3.55	3.37	3.88	3.39	3.27
186	2.05	1.91	2.18	1.8	1.4
211	0.55	0.53	0.49	0.23	0.01
240	0	0	0	0	0
272	0	0	0	0	0
310	0	0	0	0	0
352	0	0	0	0	0
400	0	0	0	0	0
454	0	0	0	0	0
516	0	0	0	0	0
586	0	0	0	0	0
666	0	0	0	0	0
756	0	0	0	0	0
859	0	0	0	0	0
976	0	0	0	0	0
1110	0	0	0	0	0
1260	0	0	0	0	0
1430	0	0	0	0	0
1630	0	0	0	0	0
1850	0	0	0	0	0
2100	0	0	0	0	0
2390	0	0	0	0	0
2710	0	0	0	0	0
3080	0	0	0	0	0
3500	0	0	0	0	0

Size (μm)	110 cm volume %	120 cm volume %	130 cm volume %	140 cm volume %	150 cm volume %
0.01	0	0	0	0	0
0.0114	0	0	0	0	0
0.0129	0	0	0	0	0
0.0147	0	0	0	0	0
0.0167	0	0	0	0	0
0.0189	0	0	0	0	0
0.0215	0	0	0	0	0
0.0244	0	0	0	0	0
0.0278	0	0	0	0	0
0.0315	0	0	0	0	0

Table 4: Continued.

0.0358	0	0	0	0	0
0.0407	0	0	0	0	0
0.0463	0	0	0	0	0
0.0526	0	0	0	0	0
0.0597	0	0	0	0	0
0.0679	0	0	0	0	0
0.0771	0	0	0	0	0
0.0876	0	0	0	0	0
0.0995	0	0	0	0	0
0.113	0	0	0	0	0
0.128	0	0	0	0	0
0.146	0	0	0	0	0
0.166	0	0	0	0	0
0.188	0	0	0	0	0
0.214	0	0	0	0	0
0.243	0	0	0	0	0
0.276	0	0	0	0	0
0.314	0	0	0	0	0
0.357	0	0	0	0	0.02
0.405	0.09	0.08	0.08	0	0.12
0.46	0.14	0.12	0.13	0.08	0.18
0.523	0.19	0.17	0.18	0.11	0.24
0.594	0.23	0.2	0.22	0.13	0.29
0.675	0.25	0.22	0.24	0.15	0.31
0.767	0.26	0.22	0.25	0.15	0.32
0.872	0.27	0.22	0.25	0.15	0.33
0.991	0.28	0.23	0.26	0.15	0.34
1.13	0.29	0.24	0.27	0.16	0.36
1.28	0.33	0.27	0.31	0.18	0.41
1.45	0.39	0.32	0.36	0.21	0.48
1.65	0.47	0.39	0.44	0.25	0.57
1.88	0.57	0.48	0.54	0.31	0.68
2.13	0.7	0.58	0.66	0.38	0.81
2.42	0.83	0.7	0.8	0.47	0.96
2.75	0.98	0.82	0.95	0.57	1.11
3.12	1.13	0.96	1.11	0.68	1.26
3.55	1.29	1.09	1.29	0.81	1.41
4.03	1.45	1.23	1.46	0.95	1.57
4.58	1.6	1.37	1.64	1.11	1.71
5.21	1.73	1.49	1.8	1.27	1.84
5.92	1.84	1.61	1.95	1.44	1.95
6.72	1.94	1.71	2.07	1.61	2.03
7.64	2.01	1.8	2.17	1.78	2.08
8.68	2.05	1.88	2.24	1.93	2.11
9.86	2.08	1.93	2.27	2.06	2.1

Table 4: Continued.

11.2	2.07	1.96	2.26	2.16	2.07
12.7	2.02	1.96	2.21	2.24	2.01
14.5	1.93	1.91	2.11	2.29	1.93
16.4	1.78	1.82	1.96	2.32	1.84
18.7	1.59	1.68	1.78	2.36	1.74
21.2	1.36	1.51	1.57	2.43	1.66
24.1	1.12	1.33	1.39	2.56	1.63
27.4	0.93	1.2	1.27	2.77	1.66
31.1	0.86	1.17	1.27	3.08	1.8
35.3	0.99	1.32	1.46	3.48	2.07
40.1	1.38	1.71	1.88	3.96	2.48
45.6	2.09	2.36	2.55	4.46	3.03
51.8	3.09	3.27	3.45	4.93	3.69
58.9	4.32	4.36	4.48	5.31	4.41
66.9	5.61	5.49	5.51	5.52	5.09
76	6.76	6.49	6.37	5.53	5.63
86.4	7.55	7.19	6.89	5.31	5.93
98.1	7.79	7.42	6.94	4.86	5.91
111	7.37	7.11	6.46	4.23	5.54
127	6.34	6.29	5.49	3.49	4.83
144	4.85	5.07	4.2	2.72	3.88
163	3.18	3.65	2.78	2	2.81
186	1.58	2.26	1.5	1.4	1.78
211	0.06	1.1	0.27	0.96	0.86
240	0	0.03	0	0.66	0.13
272	0	0	0	0.48	0
310	0	0	0	0.38	0
352	0	0	0	0.32	0
400	0	0	0	0.27	0
454	0	0	0	0.21	0
516	0	0	0	0.13	0
586	0	0	0	0.05	0
666	0	0	0	0.02	0
756	0	0	0	0	0
859	0	0	0	0	0
976	0	0	0	0	0
1110	0	0	0	0	0
1260	0	0	0	0	0
1430	0	0	0	0	0
1630	0	0	0	0	0
1850	0	0	0	0	0
2100	0	0	0	0	0
2390	0	0	0	0	0
2710	0	0	0	0	0
3080	0	0	0	0	0

Table 4: Continued.

	3500	0	0	0	0	0
Size (μm)		160 cm volume %	170 cm volume %	180 cm volume %	190 cm volume %	200 cm volume %
0.01	0	0	0	0	0	0
0.0114	0	0	0	0	0	0
0.0129	0	0	0	0	0	0
0.0147	0	0	0	0	0	0
0.0167	0	0	0	0	0	0
0.0189	0	0	0	0	0	0
0.0215	0	0	0	0	0	0
0.0244	0	0	0	0	0	0
0.0278	0	0	0	0	0	0
0.0315	0	0	0	0	0	0
0.0358	0	0	0	0	0	0
0.0407	0	0	0	0	0	0
0.0463	0	0	0	0	0	0
0.0526	0	0	0	0	0	0
0.0597	0	0	0	0	0	0
0.0679	0	0	0	0	0	0
0.0771	0	0	0	0	0	0
0.0876	0	0	0	0	0	0
0.0995	0	0	0	0	0	0
0.113	0	0	0	0	0	0
0.128	0	0	0	0	0	0
0.146	0	0	0	0	0	0
0.166	0	0	0	0	0	0
0.188	0	0	0	0	0	0
0.214	0	0	0	0	0	0
0.243	0	0	0	0	0	0
0.276	0	0	0	0	0	0
0.314	0	0	0	0	0	0
0.357	0	0	0	0	0	0
0.405	0.07	0.1	0.07	0	0.03	
0.46	0.11	0.16	0.11	0.04	0.1	
0.523	0.16	0.22	0.15	0.09	0.14	
0.594	0.19	0.26	0.18	0.11	0.17	
0.675	0.21	0.28	0.2	0.12	0.19	
0.767	0.22	0.29	0.21	0.12	0.19	
0.872	0.23	0.3	0.21	0.12	0.2	
0.991	0.23	0.3	0.22	0.13	0.2	
1.13	0.25	0.33	0.24	0.14	0.22	
1.28	0.29	0.37	0.27	0.15	0.24	
1.45	0.34	0.43	0.32	0.17	0.29	
1.65	0.41	0.52	0.38	0.2	0.34	

Table 4: Continued.

1.88	0.51	0.63	0.46	0.24	0.42
2.13	0.62	0.75	0.55	0.29	0.51
2.42	0.75	0.89	0.65	0.34	0.61
2.75	0.9	1.04	0.76	0.4	0.73
3.12	1.06	1.2	0.88	0.47	0.86
3.55	1.24	1.36	1	0.54	1
4.03	1.42	1.53	1.14	0.63	1.15
4.58	1.6	1.69	1.27	0.72	1.3
5.21	1.78	1.85	1.4	0.81	1.45
5.92	1.94	1.98	1.52	0.91	1.59
6.72	2.09	2.1	1.64	1.01	1.72
7.64	2.2	2.2	1.73	1.1	1.84
8.68	2.29	2.27	1.82	1.18	1.94
9.86	2.35	2.32	1.89	1.26	2.03
11.2	2.39	2.34	1.95	1.34	2.11
12.7	2.4	2.33	2.01	1.42	2.2
14.5	2.41	2.3	2.08	1.51	2.29
16.4	2.43	2.26	2.18	1.64	2.41
18.7	2.49	2.22	2.33	1.82	2.56
21.2	2.6	2.18	2.55	2.07	2.76
24.1	2.77	2.18	2.83	2.42	3.02
27.4	3.01	2.22	3.18	2.86	3.32
31.1	3.31	2.34	3.58	3.39	3.66
35.3	3.65	2.56	4	3.98	4.01
40.1	4	2.89	4.41	4.59	4.36
45.6	4.34	3.33	4.77	5.17	4.66
51.8	4.61	3.87	5.03	5.67	4.91
58.9	4.79	4.45	5.18	6.02	5.06
66.9	4.85	5.01	5.18	6.2	5.1
76	4.77	5.43	5.03	6.16	5
86.4	4.53	5.63	4.74	5.89	4.76
98.1	4.14	5.52	4.32	5.41	4.38
111	3.61	5.04	3.81	4.76	3.86
127	3	4.23	3.23	4	3.24
144	2.35	3.17	2.63	3.21	2.57
163	1.72	2.03	2.05	2.46	1.9
186	1.16	1.01	1.51	1.81	1.27
211	0.7	0.08	1.04	1.31	0.75
240	0.34	0	0.65	0.96	0.29
272	0.12	0	0.29	0.73	0.09
310	0.04	0	0.14	0.57	0.02
352	0	0	0.06	0.46	0
400	0	0	0.02	0.37	0
454	0	0	0	0.27	0
516	0	0	0	0.18	0

Table 4: Continued.

586	0	0	0	0.08	0
666	0	0	0	0.02	0
756	0	0	0	0	0
859	0	0	0	0	0
976	0	0	0	0	0
1110	0	0	0	0	0
1260	0	0	0	0	0
1430	0	0	0	0	0
1630	0	0	0	0	0
1850	0	0	0	0	0
2100	0	0	0	0	0
2390	0	0	0	0	0
2710	0	0	0	0	0
3080	0	0	0	0	0
3500	0	0	0	0	0
Size (μm)	210 cm volume %	220 cm volume %	230 cm volume %	240 cm volume %	250 cm volume %
0.01	0	0	0	0	0
0.0114	0	0	0	0	0
0.0129	0	0	0	0	0
0.0147	0	0	0	0	0
0.0167	0	0	0	0	0
0.0189	0	0	0	0	0
0.0215	0	0	0	0	0
0.0244	0	0	0	0	0
0.0278	0	0	0	0	0
0.0315	0	0	0	0	0
0.0358	0	0	0	0	0
0.0407	0	0	0	0	0
0.0463	0	0	0	0	0
0.0526	0	0	0	0	0
0.0597	0	0	0	0	0
0.0679	0	0	0	0	0
0.0771	0	0	0	0	0
0.0876	0	0	0	0	0
0.0995	0	0	0	0	0
0.113	0	0	0	0	0
0.128	0	0	0	0	0
0.146	0	0	0	0	0
0.166	0	0	0	0	0
0.188	0	0	0	0	0
0.214	0	0	0	0	0
0.243	0	0	0	0	0
0.276	0	0	0	0	0

Table 4: Continued.

0.314	0	0	0	0	0
0.357	0	0	0	0	0
0.405	0.07	0.04	0.04	0	0.09
0.46	0.12	0.1	0.1	0.09	0.15
0.523	0.16	0.15	0.15	0.12	0.21
0.594	0.2	0.18	0.18	0.15	0.25
0.675	0.22	0.19	0.19	0.16	0.28
0.767	0.23	0.2	0.2	0.17	0.29
0.872	0.23	0.21	0.2	0.17	0.29
0.991	0.24	0.21	0.21	0.18	0.3
1.13	0.26	0.23	0.22	0.19	0.33
1.28	0.29	0.26	0.25	0.22	0.37
1.45	0.34	0.3	0.3	0.26	0.44
1.65	0.41	0.37	0.36	0.32	0.54
1.88	0.49	0.45	0.44	0.39	0.66
2.13	0.58	0.54	0.53	0.47	0.8
2.42	0.68	0.65	0.64	0.57	0.97
2.75	0.79	0.77	0.77	0.67	1.16
3.12	0.9	0.91	0.9	0.78	1.36
3.55	1.03	1.05	1.05	0.9	1.57
4.03	1.16	1.2	1.21	1.03	1.79
4.58	1.28	1.35	1.38	1.15	2.01
5.21	1.41	1.49	1.54	1.27	2.22
5.92	1.53	1.63	1.69	1.38	2.4
6.72	1.63	1.75	1.84	1.48	2.55
7.64	1.72	1.86	1.96	1.56	2.68
8.68	1.81	1.96	2.07	1.63	2.77
9.86	1.87	2.04	2.17	1.69	2.84
11.2	1.94	2.13	2.27	1.75	2.9
12.7	2	2.22	2.37	1.82	2.95
14.5	2.08	2.33	2.49	1.9	3.01
16.4	2.19	2.47	2.65	2.02	3.09
18.7	2.34	2.65	2.87	2.19	3.2
21.2	2.55	2.89	3.15	2.41	3.35
24.1	2.83	3.17	3.48	2.69	3.53
27.4	3.17	3.49	3.86	3.03	3.71
31.1	3.55	3.84	4.24	3.41	3.89
35.3	3.94	4.19	4.58	3.81	4.04
40.1	4.33	4.5	4.85	4.2	4.12
45.6	4.66	4.74	5.01	4.56	4.13
51.8	4.9	4.9	5.02	4.85	4.04
58.9	5.03	4.94	4.89	5.06	3.87
66.9	5.02	4.86	4.61	5.16	3.61
76	4.86	4.65	4.21	5.12	3.28
86.4	4.56	4.32	3.72	4.95	2.88

Table 4: Continued.

98.1	4.14	3.88	3.18	4.63	2.45
111	3.61	3.38	2.64	4.19	2
127	3.03	2.83	2.13	3.66	1.58
144	2.45	2.29	1.69	3.06	1.21
163	1.91	1.78	1.34	2.47	0.91
186	1.45	1.32	1.08	1.91	0.69
211	1.08	0.94	0.89	1.42	0.54
240	0.8	0.63	0.74	1.01	0.44
272	0.59	0.36	0.6	0.69	0.38
310	0.44	0.16	0.45	0.44	0.31
352	0.32	0.05	0.28	0.25	0.24
400	0.23	0.01	0.13	0.14	0.16
454	0.16	0	0	0.1	0.09
516	0.08	0	0	0.05	0.05
586	0.07	0	0	0.02	0.02
666	0.04	0	0	0	0
756	0.02	0	0	0	0
859	0	0	0	0	0
976	0	0	0	0	0
1110	0	0	0	0	0
1260	0	0	0	0	0
1430	0	0	0	0	0
1630	0	0	0	0	0
1850	0	0	0	0	0
2100	0	0	0	0	0
2390	0	0	0	0	0
2710	0	0	0	0	0
3080	0	0	0	0	0
3500	0	0	0	0	0

Size (μm)	260 cm volume %	270 cm volume %	280 cm volume %	290 cm volume %	300 cm volume %
0.01	0	0	0	0	0
0.0114	0	0	0	0	0
0.0129	0	0	0	0	0
0.0147	0	0	0	0	0
0.0167	0	0	0	0	0
0.0189	0	0	0	0	0
0.0215	0	0	0	0	0
0.0244	0	0	0	0	0
0.0278	0	0	0	0	0
0.0315	0	0	0	0	0
0.0358	0	0	0	0	0
0.0407	0	0	0	0	0
0.0463	0	0	0	0	0

Table 4: Continued.

0.0526	0	0	0	0	0
0.0597	0	0	0	0	0
0.0679	0	0	0	0	0
0.0771	0	0	0	0	0
0.0876	0	0	0	0	0
0.0995	0	0	0	0	0
0.113	0	0	0	0	0
0.128	0	0	0	0	0
0.146	0	0	0	0	0
0.166	0	0	0	0	0
0.188	0	0	0	0	0
0.214	0	0	0	0	0
0.243	0	0	0	0	0
0.276	0	0	0	0	0
0.314	0	0	0.08	0	0
0.357	0.09	0.05	0.21	0	0
0.405	0.18	0.13	0.39	0	0
0.46	0.28	0.21	0.56	0.07	0.08
0.523	0.36	0.28	0.72	0.1	0.12
0.594	0.42	0.34	0.83	0.12	0.14
0.675	0.45	0.37	0.89	0.13	0.16
0.767	0.46	0.38	0.92	0.14	0.16
0.872	0.47	0.39	0.95	0.14	0.16
0.991	0.49	0.4	1	0.15	0.17
1.13	0.53	0.43	1.09	0.16	0.18
1.28	0.6	0.49	1.24	0.18	0.2
1.45	0.71	0.58	1.45	0.21	0.23
1.65	0.86	0.71	1.71	0.25	0.28
1.88	1.04	0.87	2.01	0.29	0.33
2.13	1.24	1.06	2.32	0.34	0.4
2.42	1.46	1.28	2.62	0.39	0.47
2.75	1.68	1.5	2.88	0.45	0.56
3.12	1.9	1.74	3.09	0.51	0.65
3.55	2.12	1.98	3.25	0.58	0.75
4.03	2.31	2.23	3.37	0.65	0.86
4.58	2.49	2.45	3.45	0.73	0.98
5.21	2.63	2.65	3.47	0.81	1.09
5.92	2.73	2.82	3.45	0.88	1.2
6.72	2.79	2.94	3.39	0.96	1.3
7.64	2.81	3.01	3.28	1.03	1.39
8.68	2.79	3.05	3.15	1.09	1.46
9.86	2.76	3.04	3	1.15	1.53
11.2	2.72	3.02	2.83	1.23	1.6
12.7	2.69	2.98	2.66	1.32	1.68
14.5	2.69	2.95	2.48	1.47	1.81

Table 4: Continued.

16.4	2.72	2.94	2.31	1.69	2
18.7	2.79	2.97	2.17	2.03	2.3
21.2	2.91	3.04	2.05	2.49	2.71
24.1	3.06	3.15	1.97	3.08	3.23
27.4	3.22	3.28	1.93	3.79	3.86
31.1	3.36	3.42	1.91	4.57	4.54
35.3	3.47	3.53	1.9	5.35	5.21
40.1	3.52	3.6	1.9	6.04	5.8
45.6	3.5	3.6	1.89	6.56	6.24
51.8	3.4	3.53	1.86	6.83	6.45
58.9	3.23	3.38	1.81	6.81	6.42
66.9	3	3.18	1.73	6.49	6.12
76	2.72	2.92	1.61	5.9	5.59
86.4	2.4	2.63	1.47	5.1	4.88
98.1	2.08	2.31	1.32	4.2	4.07
111	1.76	2	1.17	3.28	3.24
127	1.48	1.68	1.03	2.44	2.45
144	1.24	1.38	0.92	1.74	1.77
163	1.06	1.09	0.85	1.21	1.21
186	0.92	0.82	0.8	0.86	0.79
211	0.82	0.57	0.78	0.67	0.44
240	0.72	0.33	0.77	0.58	0.27
272	0.62	0.19	0.74	0.53	0.17
310	0.49	0.1	0.68	0.49	0.11
352	0.34	0.03	0.59	0.43	0.08
400	0.22	0	0.45	0.35	0.06
454	0.13	0	0.32	0.26	0.03
516	0.07	0	0.2	0.19	0
586	0.01	0	0.09	0.14	0
666	0	0	0.02	0.1	0
756	0	0	0	0.07	0
859	0	0	0	0.03	0
976	0	0	0	0.02	0
1110	0	0	0	0.02	0
1260	0	0	0	0.02	0
1430	0	0	0	0.02	0
1630	0	0	0	0.02	0
1850	0	0	0	0.02	0
2100	0	0	0	0.01	0
2390	0	0	0	0	0
2710	0	0	0	0	0
3080	0	0	0	0	0
3500	0	0	0	0	0

Table 4: Continued.

Size (μm)	310 cm volume %	320 cm volume %	330 cm volume %	340 cm volume %	350 cm volume %
0.01	0	0	0	0	0
0.0114	0	0	0	0	0
0.0129	0	0	0	0	0
0.0147	0	0	0	0	0
0.0167	0	0	0	0	0
0.0189	0	0	0	0	0
0.0215	0	0	0	0	0
0.0244	0	0	0	0	0
0.0278	0	0	0	0	0
0.0315	0	0	0	0	0
0.0358	0	0	0	0	0
0.0407	0	0	0	0	0
0.0463	0	0	0	0	0
0.0526	0	0	0	0	0
0.0597	0	0	0	0	0
0.0679	0	0	0	0	0
0.0771	0	0	0	0	0
0.0876	0	0	0	0	0
0.0995	0	0	0	0	0
0.113	0	0	0	0	0
0.128	0	0	0	0	0
0.146	0	0	0	0	0
0.166	0	0	0	0	0
0.188	0	0	0	0	0
0.214	0	0	0	0	0
0.243	0	0	0	0	0
0.276	0	0	0	0	0
0.314	0	0	0	0	0
0.357	0	0	0.09	0	0
0.405	0.07	0.08	0.18	0.07	0
0.46	0.11	0.13	0.28	0.12	0.07
0.523	0.16	0.18	0.37	0.16	0.1
0.594	0.19	0.22	0.44	0.19	0.12
0.675	0.2	0.24	0.48	0.21	0.13
0.767	0.21	0.25	0.5	0.22	0.13
0.872	0.22	0.26	0.51	0.22	0.13
0.991	0.22	0.26	0.53	0.23	0.13
1.13	0.24	0.28	0.57	0.25	0.14
1.28	0.27	0.32	0.65	0.28	0.16
1.45	0.32	0.37	0.75	0.33	0.19
1.65	0.38	0.44	0.89	0.4	0.22
1.88	0.46	0.53	1.05	0.47	0.26

Table 4: Continued.

2.13	0.55	0.64	1.23	0.56	0.3
2.42	0.65	0.76	1.41	0.66	0.35
2.75	0.75	0.89	1.59	0.76	0.41
3.12	0.87	1.04	1.77	0.87	0.48
3.55	0.99	1.2	1.93	0.98	0.56
4.03	1.11	1.37	2.08	1.1	0.64
4.58	1.24	1.55	2.22	1.21	0.74
5.21	1.36	1.73	2.34	1.32	0.84
5.92	1.47	1.9	2.42	1.43	0.93
6.72	1.56	2.05	2.48	1.52	1.02
7.64	1.64	2.18	2.52	1.59	1.09
8.68	1.71	2.27	2.52	1.65	1.15
9.86	1.76	2.33	2.49	1.7	1.2
11.2	1.8	2.36	2.44	1.74	1.24
12.7	1.86	2.38	2.36	1.78	1.3
14.5	1.95	2.42	2.27	1.86	1.41
16.4	2.1	2.5	2.19	1.99	1.62
18.7	2.34	2.66	2.13	2.2	1.95
21.2	2.67	2.92	2.13	2.52	2.45
24.1	3.11	3.3	2.21	2.96	3.1
27.4	3.64	3.78	2.4	3.5	3.89
31.1	4.22	4.32	2.7	4.12	4.75
35.3	4.8	4.85	3.11	4.75	5.58
40.1	5.3	5.29	3.58	5.34	6.29
45.6	5.65	5.57	4.06	5.79	6.75
51.8	5.81	5.62	4.48	6.04	6.91
58.9	5.74	5.41	4.75	6.04	6.73
66.9	5.45	4.97	4.81	5.79	6.22
76	4.96	4.35	4.62	5.31	5.47
86.4	4.33	3.61	4.18	4.64	4.58
98.1	3.64	2.85	3.55	3.87	3.66
111	2.97	2.15	2.81	3.09	2.8
127	2.36	1.56	2.05	2.36	2.09
144	1.85	1.11	1.37	1.74	1.56
163	1.45	0.8	0.82	1.26	1.22
186	1.13	0.6	0.4	0.91	1.03
211	0.87	0.46	0.19	0.67	0.94
240	0.63	0.34	0.07	0.49	0.91
272	0.39	0.22	0.01	0.35	0.87
310	0.2	0.09	0	0.22	0.81
352	0.06	0.02	0	0.11	0.71
400	0	0	0	0.04	0.58
454	0	0	0	0.02	0.44
516	0	0	0	0	0.29
586	0	0	0	0	0.19

Table 4: Continued.

666	0	0	0	0	0.11
756	0	0	0	0	0.06
859	0	0	0	0	0.02
976	0	0	0	0	0
1110	0	0	0	0	0
1260	0	0	0	0	0
1430	0	0	0	0	0
1630	0	0	0	0	0
1850	0	0	0	0	0
2100	0	0	0	0	0
2390	0	0	0	0	0
2710	0	0	0	0	0
3080	0	0	0	0	0
3500	0	0	0	0	0
Size (μm)	360 cm	370 cm			
	volume %	volume %			
0.01	0	0			
0.0114	0	0			
0.0129	0	0			
0.0147	0	0			
0.0167	0	0			
0.0189	0	0			
0.0215	0	0			
0.0244	0	0			
0.0278	0	0			
0.0315	0	0			
0.0358	0	0			
0.0407	0	0			
0.0463	0	0			
0.0526	0	0			
0.0597	0	0			
0.0679	0	0			
0.0771	0	0			
0.0876	0	0			
0.0995	0	0			
0.113	0	0			
0.128	0	0			
0.146	0	0			
0.166	0	0			
0.188	0	0			
0.214	0	0			
0.243	0	0			
0.276	0	0			
0.314	0	0			

Table 4: Continued.

0.357	0	0.1
0.405	0.09	0.21
0.46	0.14	0.32
0.523	0.19	0.42
0.594	0.23	0.49
0.675	0.25	0.53
0.767	0.26	0.55
0.872	0.27	0.57
0.991	0.27	0.59
1.13	0.29	0.64
1.28	0.33	0.72
1.45	0.38	0.84
1.65	0.45	0.99
1.88	0.53	1.18
2.13	0.63	1.38
2.42	0.74	1.6
2.75	0.87	1.81
3.12	1.01	2.02
3.55	1.16	2.22
4.03	1.32	2.4
4.58	1.48	2.56
5.21	1.64	2.69
5.92	1.77	2.78
6.72	1.89	2.83
7.64	1.98	2.84
8.68	2.04	2.81
9.86	2.09	2.76
11.2	2.14	2.68
12.7	2.22	2.6
14.5	2.37	2.53
16.4	2.62	2.5
18.7	2.98	2.52
21.2	3.47	2.6
24.1	4.04	2.75
27.4	4.66	2.96
31.1	5.23	3.2
35.3	5.68	3.44
40.1	5.93	3.64
45.6	5.92	3.77
51.8	5.65	3.79
58.9	5.13	3.69
66.9	4.44	3.47
76	3.66	3.15
86.4	2.87	2.76
98.1	2.16	2.34

Table 4: Continued.

111	1.58	1.91
127	1.14	1.51
144	0.84	1.16
163	0.66	0.85
186	0.56	0.59
211	0.49	0.37
240	0.43	0.18
272	0.34	0.09
310	0.24	0.07
352	0.15	0.04
400	0.08	0.01
454	0.02	0
516	0	0
586	0	0
666	0	0
756	0	0
859	0	0
976	0	0
1110	0	0
1260	0	0
1430	0	0
1630	0	0
1850	0	0
2100	0	0
2390	0	0
2710	0	0
3080	0	0
3500	0	0

Table 5: CB 2-2 grain size distributions vs. depth.

Size (μm)	10 cm	20 cm	30 cm	40cm	50 cm
	volume %				
0.01	0	0	0	0	0
0.0114	0	0	0	0	0
0.0129	0	0	0	0	0
0.0147	0	0	0	0	0
0.0167	0	0	0	0	0
0.0189	0	0	0	0	0
0.0215	0	0	0	0	0
0.0244	0	0	0	0	0
0.0278	0	0	0	0	0
0.0315	0	0	0	0	0
0.0358	0	0	0	0	0

Table 5: Continued.

0.0407	0	0	0	0	0
0.0463	0	0	0	0	0
0.0526	0	0	0	0	0
0.0597	0	0	0	0	0
0.0679	0	0	0	0	0
0.0771	0	0	0	0	0
0.0876	0	0	0	0	0
0.0995	0	0	0	0	0
0.113	0	0	0	0	0
0.128	0	0	0	0	0
0.146	0	0	0	0	0
0.166	0	0	0	0	0
0.188	0	0	0	0	0
0.214	0	0	0	0	0
0.243	0	0.01	0	0	0
0.276	0.11	0.19	0.09	0.1	0
0.314	0.32	0.49	0.31	0.33	0.18
0.357	0.59	0.89	0.64	0.67	0.39
0.405	0.88	1.29	0.99	1.04	0.62
0.46	1.13	1.63	1.32	1.38	0.83
0.523	1.3	1.87	1.57	1.64	0.99
0.594	1.4	1.99	1.72	1.8	1.09
0.675	1.43	2.02	1.79	1.87	1.13
0.767	1.41	1.98	1.8	1.89	1.14
0.872	1.39	1.94	1.81	1.9	1.16
0.991	1.4	1.94	1.86	1.96	1.2
1.13	1.47	2.01	1.96	2.07	1.29
1.28	1.59	2.16	2.14	2.26	1.43
1.45	1.78	2.38	2.38	2.51	1.62
1.65	2	2.66	2.67	2.79	1.84
1.88	2.25	2.95	2.97	3.07	2.08
2.13	2.48	3.2	3.24	3.31	2.29
2.42	2.64	3.38	3.44	3.48	2.47
2.75	2.73	3.46	3.55	3.56	2.59
3.12	2.73	3.43	3.57	3.56	2.65
3.55	2.67	3.32	3.51	3.51	2.66
4.03	2.57	3.17	3.41	3.42	2.63
4.58	2.45	2.98	3.27	3.31	2.57
5.21	2.32	2.78	3.11	3.18	2.47
5.92	2.19	2.57	2.92	3.05	2.34
6.72	2.06	2.37	2.72	2.91	2.21
7.64	1.95	2.18	2.52	2.76	2.06
8.68	1.85	2.01	2.32	2.6	1.93
9.86	1.75	1.85	2.13	2.44	1.81
11.2	1.67	1.71	1.95	2.27	1.7

Table 5: Continued.

12.7	1.58	1.59	1.78	2.1	1.61
14.5	1.48	1.48	1.63	1.92	1.53
16.4	1.39	1.39	1.51	1.74	1.47
18.7	1.28	1.32	1.41	1.57	1.4
21.2	1.18	1.26	1.35	1.42	1.33
24.1	1.07	1.21	1.3	1.29	1.26
27.4	0.97	1.17	1.28	1.17	1.17
31.1	0.88	1.13	1.26	1.07	1.08
35.3	0.8	1.08	1.25	0.98	1.01
40.1	0.73	1.03	1.23	0.92	1
45.6	0.7	0.99	1.22	0.88	1.06
51.8	0.69	0.96	1.2	0.88	1.24
58.9	0.73	0.94	1.18	0.92	1.55
66.9	0.81	0.95	1.17	1	1.99
76	0.93	0.97	1.17	1.12	2.51
86.4	1.08	1	1.17	1.26	3.06
98.1	1.26	1.01	1.17	1.38	3.53
111	1.44	1	1.17	1.45	3.86
127	1.61	0.95	1.16	1.44	3.97
144	1.74	0.86	1.14	1.34	3.83
163	1.82	0.73	1.1	1.14	3.47
186	1.84	0.59	1.04	0.88	2.91
211	1.8	0.45	0.97	0.6	2.22
240	1.71	0.33	0.89	0.32	1.5
272	1.58	0.33	0.78	0.13	0.76
310	1.45	0.36	0.64	0.07	0.26
352	1.32	0.41	0.48	0.07	0.05
400	1.23	0.47	0.32	0.08	0
454	1.17	0.53	0.18	0.07	0
516	1.14	0.59	0.08	0.07	0
586	1.13	0.64	0.04	0.05	0
666	1.1	0.66	0.02	0.03	0
756	1.11	0.66	0.02	0.02	0
859	1.07	0.63	0.01	0	0
976	0.99	0.59	0	0	0
1110	0.88	0.54	0	0	0
1260	0.78	0.49	0	0	0
1430	0.72	0.45	0	0	0
1630	0.64	0.39	0	0	0
1850	0.55	0.34	0	0	0
2100	0.45	0.28	0	0	0
2390	0.34	0.21	0	0	0
2710	0.23	0.14	0	0	0
3080	0.12	0.07	0	0	0
3500	0	0	0	0	0

Table 5: Continued.

Size (μm)	60 cm volume %	70 cm volume %	80 cm volume %	90 cm volume %	100 cm volume %
0.01	0	0	0	0	0
0.0114	0	0	0	0	0
0.0129	0	0	0	0	0
0.0147	0	0	0	0	0
0.0167	0	0	0	0	0
0.0189	0	0	0	0	0
0.0215	0	0	0	0	0
0.0244	0	0	0	0	0
0.0278	0	0	0	0	0
0.0315	0	0	0	0	0
0.0358	0	0	0	0	0
0.0407	0	0	0	0	0
0.0463	0	0	0	0	0
0.0526	0	0	0	0	0
0.0597	0	0	0	0	0
0.0679	0	0	0	0	0
0.0771	0	0	0	0	0
0.0876	0	0	0	0	0
0.0995	0	0	0	0	0
0.113	0	0	0	0	0
0.128	0	0	0	0	0
0.146	0	0	0	0	0
0.166	0	0	0	0	0
0.188	0	0	0	0	0
0.214	0	0	0	0	0
0.243	0	0	0	0	0
0.276	0	0.1	0	0	0
0.314	0.15	0.28	0.05	0	0.15
0.357	0.3	0.53	0.13	0.11	0.33
0.405	0.47	0.79	0.2	0.22	0.54
0.46	0.62	1	0.26	0.34	0.73
0.523	0.73	1.16	0.31	0.45	0.88
0.594	0.79	1.23	0.33	0.53	0.97
0.675	0.82	1.24	0.34	0.57	1.01
0.767	0.83	1.22	0.33	0.59	1.02
0.872	0.83	1.2	0.33	0.61	1.03
0.991	0.85	1.21	0.34	0.64	1.06
1.13	0.91	1.28	0.36	0.71	1.14
1.28	0.99	1.41	0.4	0.83	1.27
1.45	1.11	1.6	0.46	1.01	1.45
1.65	1.25	1.83	0.52	1.24	1.68
1.88	1.39	2.09	0.59	1.52	1.93

Table 5: Continued.

2.13	1.53	2.33	0.66	1.84	2.17
2.42	1.63	2.53	0.71	2.17	2.39
2.75	1.7	2.67	0.75	2.5	2.56
3.12	1.72	2.76	0.77	2.82	2.67
3.55	1.72	2.79	0.77	3.11	2.74
4.03	1.7	2.78	0.77	3.36	2.77
4.58	1.66	2.74	0.75	3.57	2.76
5.21	1.6	2.66	0.73	3.7	2.72
5.92	1.53	2.57	0.7	3.77	2.65
6.72	1.46	2.46	0.67	3.77	2.56
7.64	1.38	2.33	0.63	3.69	2.45
8.68	1.3	2.2	0.59	3.57	2.32
9.86	1.23	2.07	0.55	3.4	2.2
11.2	1.16	1.94	0.52	3.21	2.06
12.7	1.1	1.82	0.49	2.99	1.93
14.5	1.04	1.7	0.46	2.78	1.81
16.4	0.99	1.6	0.44	2.58	1.7
18.7	0.94	1.51	0.43	2.39	1.61
21.2	0.9	1.45	0.42	2.23	1.53
24.1	0.86	1.39	0.41	2.1	1.48
27.4	0.83	1.35	0.4	1.98	1.43
31.1	0.8	1.32	0.4	1.88	1.39
35.3	0.78	1.3	0.4	1.8	1.35
40.1	0.77	1.28	0.41	1.74	1.32
45.6	0.79	1.27	0.44	1.7	1.3
51.8	0.83	1.28	0.51	1.71	1.31
58.9	0.9	1.31	0.62	1.75	1.36
66.9	1.01	1.36	0.79	1.84	1.47
76	1.15	1.43	1	1.96	1.62
86.4	1.3	1.5	1.26	2.08	1.81
98.1	1.45	1.57	1.53	2.16	1.99
111	1.58	1.62	1.78	2.15	2.13
127	1.66	1.62	1.96	2.04	2.17
144	1.7	1.58	2.05	1.8	2.07
163	1.7	1.49	2.03	1.46	1.84
186	1.66	1.37	1.91	1.08	1.49
211	1.6	1.24	1.74	0.7	1.08
240	1.54	1.12	1.57	0.52	0.68
272	1.49	1.01	1.5	0.36	0.42
310	1.45	0.93	1.58	0.2	0.31
352	1.45	0.89	1.88	0.11	0.33
400	1.49	0.87	2.42	0.02	0.52
454	1.58	0.87	3.17	0	0.82
516	1.72	0.86	4.03	0	1.16
586	1.89	0.84	4.88	0	1.48

Table 5: Continued.

666	2.08	0.81	5.56	0	1.66
756	2.28	0.77	5.92	0	1.64
859	2.46	0.7	5.9	0	1.42
976	2.61	0.63	5.49	0	1.07
1110	2.7	0.58	4.75	0	0.7
1260	2.71	0.54	4.04	0	0.34
1430	2.7	0.49	3.26	0	0
1630	2.57	0.45	2.51	0	0
1850	2.34	0.4	1.88	0	0
2100	2	0.34	1.37	0	0
2390	1.58	0.27	0.96	0	0
2710	1.09	0.18	0.61	0	0
3080	0.56	0.09	0.3	0	0
3500	0	0	0	0	0
Size (μm)	110 cm volume %	120 cm volume %	130 cm volume %	140 cm volume %	150 cm volume %
0.01	0	0	0	0	0
0.0114	0	0	0	0	0
0.0129	0	0	0	0	0
0.0147	0	0	0	0	0
0.0167	0	0	0	0	0
0.0189	0	0	0	0	0
0.0215	0	0	0	0	0
0.0244	0	0	0	0	0
0.0278	0	0	0	0	0
0.0315	0	0	0	0	0
0.0358	0	0	0	0	0
0.0407	0	0	0	0	0
0.0463	0	0	0	0	0
0.0526	0	0	0	0	0
0.0597	0	0	0	0	0
0.0679	0	0	0	0	0
0.0771	0	0	0	0	0
0.0876	0	0	0	0	0
0.0995	0	0	0	0	0
0.113	0	0	0	0	0
0.128	0	0	0	0	0
0.146	0	0	0	0	0
0.166	0	0	0	0	0
0.188	0	0	0	0	0
0.214	0	0	0	0	0
0.243	0	0	0	0	0
0.276	0.07	0	0.04	0	0
0.314	0.25	0.14	0.22	0	0.16

Table 5: Continued.

0.357	0.48	0.29	0.43	0.09	0.34
0.405	0.72	0.46	0.67	0.18	0.55
0.46	0.94	0.63	0.88	0.27	0.76
0.523	1.09	0.75	1.04	0.36	0.91
0.594	1.16	0.83	1.12	0.42	1.02
0.675	1.18	0.87	1.16	0.46	1.07
0.767	1.17	0.88	1.15	0.48	1.08
0.872	1.16	0.89	1.15	0.49	1.09
0.991	1.19	0.92	1.18	0.51	1.13
1.13	1.26	0.98	1.26	0.56	1.2
1.28	1.38	1.08	1.38	0.65	1.33
1.45	1.54	1.21	1.55	0.77	1.51
1.65	1.71	1.37	1.75	0.94	1.73
1.88	1.88	1.54	1.95	1.13	1.98
2.13	2.03	1.7	2.13	1.36	2.21
2.42	2.14	1.82	2.27	1.59	2.42
2.75	2.21	1.91	2.36	1.83	2.58
3.12	2.23	1.95	2.4	2.06	2.68
3.55	2.22	1.97	2.41	2.28	2.74
4.03	2.2	1.95	2.39	2.48	2.77
4.58	2.17	1.93	2.35	2.66	2.76
5.21	2.13	1.88	2.29	2.79	2.73
5.92	2.08	1.82	2.22	2.88	2.67
6.72	2.02	1.76	2.13	2.91	2.59
7.64	1.95	1.69	2.04	2.9	2.49
8.68	1.88	1.63	1.94	2.85	2.38
9.86	1.8	1.57	1.83	2.76	2.27
11.2	1.71	1.51	1.73	2.64	2.15
12.7	1.64	1.47	1.62	2.51	2.04
14.5	1.57	1.43	1.53	2.37	1.93
16.4	1.53	1.41	1.44	2.25	1.84
18.7	1.53	1.39	1.38	2.15	1.77
21.2	1.57	1.39	1.35	2.09	1.73
24.1	1.65	1.41	1.33	2.07	1.7
27.4	1.77	1.44	1.34	2.08	1.69
31.1	1.91	1.49	1.36	2.13	1.69
35.3	2.04	1.56	1.38	2.19	1.69
40.1	2.16	1.67	1.41	2.26	1.69
45.6	2.23	1.83	1.44	2.32	1.69
51.8	2.25	2.03	1.48	2.37	1.71
58.9	2.21	2.26	1.52	2.41	1.74
66.9	2.14	2.51	1.58	2.43	1.79
76	2.03	2.72	1.64	2.44	1.86
86.4	1.91	2.87	1.7	2.44	1.94
98.1	1.78	2.92	1.74	2.43	2.01

Table 5: Continued.

111	1.65	2.84	1.75	2.4	2.05
127	1.54	2.63	1.72	2.35	2.03
144	1.43	2.32	1.63	2.28	1.94
163	1.32	1.95	1.51	2.18	1.8
186	1.21	1.57	1.36	2.06	1.61
211	1.09	1.25	1.22	1.91	1.41
240	0.95	1	1.1	1.72	1.23
272	0.79	0.86	1.02	1.49	1.09
310	0.61	0.81	0.99	1.21	0.98
352	0.43	0.83	1.01	0.9	0.91
400	0.32	0.91	1.1	0.59	0.84
454	0.2	0.97	1.23	0.3	0.76
516	0.11	1	1.33	0.14	0.63
586	0.08	0.98	1.38	0.11	0.47
666	0.16	0.92	1.37	0.08	0.29
756	0.3	0.84	1.31	0.04	0.12
859	0.51	0.82	1.19	0.01	0.02
976	0.75	0.84	1.04	0	0
1110	0.98	0.9	0.91	0	0
1260	1.16	0.99	0.79	0	0
1430	1.26	1.03	0.66	0	0
1630	1.28	1.01	0.53	0	0
1850	1.21	0.93	0.42	0	0
2100	1.06	0.8	0.32	0	0
2390	0.85	0.63	0.23	0	0
2710	0.59	0.43	0.14	0	0
3080	0.31	0.21	0.07	0	0
3500	0	0	0	0	0

Size (μm)	160 cm volume %	170 cm volume %	180 cm volume %	190 cm volume %	200 cm volume %
0.01	0	0	0	0	0
0.0114	0	0	0	0	0
0.0129	0	0	0	0	0
0.0147	0	0	0	0	0
0.0167	0	0	0	0	0
0.0189	0	0	0	0	0
0.0215	0	0	0	0	0
0.0244	0	0	0	0	0
0.0278	0	0	0	0	0
0.0315	0	0	0	0	0
0.0358	0	0	0	0	0
0.0407	0	0	0	0	0
0.0463	0	0	0	0	0
0.0526	0	0	0	0	0

Table 5: Continued.

0.0597	0	0	0	0	0
0.0679	0	0	0	0	0
0.0771	0	0	0	0	0
0.0876	0	0	0	0	0
0.0995	0	0	0	0	0
0.113	0	0	0	0	0
0.128	0	0	0	0	0
0.146	0	0	0	0	0
0.166	0	0	0	0	0
0.188	0	0	0	0	0
0.214	0	0	0	0	0
0.243	0	0	0	0	0
0.276	0	0	0	0	0
0.314	0.17	0.12	0	0	0
0.357	0.37	0.28	0.09	0.07	0.12
0.405	0.59	0.46	0.19	0.16	0.23
0.46	0.79	0.65	0.29	0.26	0.34
0.523	0.95	0.8	0.38	0.36	0.45
0.594	1.05	0.9	0.44	0.44	0.52
0.675	1.1	0.96	0.48	0.5	0.57
0.767	1.12	0.99	0.5	0.55	0.6
0.872	1.14	1.02	0.51	0.58	0.63
0.991	1.17	1.06	0.54	0.63	0.67
1.13	1.24	1.14	0.59	0.7	0.74
1.28	1.36	1.27	0.68	0.8	0.85
1.45	1.51	1.43	0.8	0.93	1.01
1.65	1.69	1.63	0.95	1.09	1.2
1.88	1.88	1.84	1.13	1.27	1.42
2.13	2.05	2.03	1.33	1.46	1.65
2.42	2.18	2.2	1.53	1.66	1.87
2.75	2.26	2.31	1.72	1.86	2.06
3.12	2.29	2.38	1.89	2.05	2.22
3.55	2.29	2.41	2.05	2.23	2.35
4.03	2.26	2.41	2.19	2.38	2.44
4.58	2.22	2.37	2.31	2.5	2.48
5.21	2.16	2.32	2.39	2.57	2.48
5.92	2.09	2.24	2.44	2.6	2.44
6.72	2	2.15	2.46	2.58	2.36
7.64	1.91	2.04	2.45	2.52	2.26
8.68	1.82	1.93	2.42	2.44	2.15
9.86	1.72	1.83	2.36	2.33	2.03
11.2	1.63	1.72	2.3	2.22	1.92
12.7	1.54	1.62	2.24	2.1	1.81
14.5	1.46	1.54	2.17	1.97	1.7
16.4	1.4	1.47	2.12	1.84	1.6

Table 5: Continued.

	210 cm volume %	220 cm volume %	230 cm volume %	240 cm volume %	250 cm volume %
Size (μm)					
18.7	1.36	1.41	2.08	1.69	1.48
21.2	1.34	1.38	2.05	1.52	1.36
24.1	1.34	1.37	2.05	1.32	1.23
27.4	1.37	1.38	2.07	1.1	1.1
31.1	1.41	1.4	2.11	0.87	0.99
35.3	1.47	1.44	2.17	0.67	0.94
40.1	1.54	1.49	2.25	0.57	0.99
45.6	1.61	1.56	2.36	0.62	1.18
51.8	1.69	1.66	2.49	0.88	1.54
58.9	1.78	1.78	2.65	1.4	2.07
66.9	1.88	1.93	2.82	2.15	2.72
76	1.98	2.09	2.98	3.06	3.42
86.4	2.08	2.24	3.11	4.02	4.05
98.1	2.16	2.36	3.17	4.87	4.51
111	2.21	2.42	3.14	5.44	4.7
127	2.22	2.41	3.01	5.61	4.58
144	2.19	2.33	2.78	5.34	4.15
163	2.13	2.19	2.48	4.66	3.51
186	2.06	2.03	2.14	3.69	2.75
211	1.99	1.89	1.81	2.6	2
240	1.94	1.79	1.51	1.57	1.36
272	1.92	1.74	1.26	0.69	0.88
310	1.91	1.72	1.04	0.01	0.57
352	1.88	1.69	0.85	0	0.39
400	1.81	1.62	0.67	0	0.37
454	1.66	1.48	0.47	0	0.37
516	1.41	1.26	0.3	0	0.36
586	1.05	0.97	0.17	0	0.33
666	0.7	0.68	0.06	0	0.28
756	0.37	0.42	0	0	0.23
859	0.13	0.22	0	0	0.19
976	0.01	0.1	0	0	0.14
1110	0	0.04	0	0	0.08
1260	0	0	0	0	0.02
1430	0	0	0	0	0
1630	0	0	0	0	0
1850	0	0	0	0	0
2100	0	0	0	0	0
2390	0	0	0	0	0
2710	0	0	0	0	0
3080	0	0	0	0	0
3500	0	0	0	0	0

Table 5: Continued.

0.01	0	0	0	0	0
0.0114	0	0	0	0	0
0.0129	0	0	0	0	0
0.0147	0	0	0	0	0
0.0167	0	0	0	0	0
0.0189	0	0	0	0	0
0.0215	0	0	0	0	0
0.0244	0	0	0	0	0
0.0278	0	0	0	0	0
0.0315	0	0	0	0	0
0.0358	0	0	0	0	0
0.0407	0	0	0	0	0
0.0463	0	0	0	0	0
0.0526	0	0	0	0	0
0.0597	0	0	0	0	0
0.0679	0	0	0	0	0
0.0771	0	0	0	0	0
0.0876	0	0	0	0	0
0.0995	0	0	0	0	0
0.113	0	0	0	0	0
0.128	0	0	0	0	0
0.146	0	0	0	0	0
0.166	0	0	0	0	0
0.188	0	0	0	0	0
0.214	0	0	0	0	0
0.243	0	0	0	0	0
0.276	0	0	0	0	0
0.314	0	0	0	0	0.07
0.357	0.13	0.07	0.13	0.09	0.17
0.405	0.24	0.14	0.25	0.18	0.31
0.46	0.36	0.22	0.37	0.28	0.44
0.523	0.45	0.29	0.47	0.36	0.56
0.594	0.53	0.34	0.55	0.43	0.63
0.675	0.57	0.37	0.59	0.47	0.68
0.767	0.6	0.39	0.61	0.49	0.7
0.872	0.62	0.4	0.63	0.51	0.72
0.991	0.66	0.42	0.66	0.54	0.76
1.13	0.72	0.46	0.71	0.6	0.83
1.28	0.81	0.52	0.81	0.69	0.94
1.45	0.94	0.61	0.94	0.81	1.08
1.65	1.1	0.74	1.1	0.98	1.27
1.88	1.28	0.89	1.3	1.17	1.47
2.13	1.46	1.05	1.5	1.37	1.69
2.42	1.63	1.23	1.71	1.58	1.88
2.75	1.77	1.41	1.9	1.77	2.06

Table 5: Continued.

3.12	1.87	1.58	2.06	1.95	2.19
3.55	1.94	1.74	2.21	2.1	2.29
4.03	1.98	1.89	2.33	2.23	2.36
4.58	1.99	2.02	2.42	2.32	2.4
5.21	1.97	2.11	2.47	2.38	2.39
5.92	1.92	2.18	2.5	2.41	2.36
6.72	1.85	2.21	2.49	2.4	2.3
7.64	1.77	2.23	2.47	2.37	2.22
8.68	1.68	2.22	2.42	2.32	2.13
9.86	1.59	2.21	2.37	2.26	2.03
11.2	1.51	2.18	2.31	2.2	1.94
12.7	1.44	2.15	2.24	2.13	1.85
14.5	1.37	2.11	2.15	2.06	1.75
16.4	1.3	2.03	2.04	1.98	1.65
18.7	1.22	1.92	1.91	1.89	1.55
21.2	1.12	1.76	1.74	1.79	1.44
24.1	1	1.56	1.55	1.7	1.33
27.4	0.87	1.33	1.36	1.63	1.23
31.1	0.74	1.1	1.21	1.59	1.15
35.3	0.65	0.96	1.15	1.63	1.12
40.1	0.65	0.96	1.22	1.75	1.17
45.6	0.78	1.17	1.47	1.99	1.32
51.8	1.11	1.66	1.92	2.33	1.59
58.9	1.63	2.4	2.53	2.75	1.97
66.9	2.34	3.36	3.24	3.19	2.41
76	3.18	4.38	3.94	3.57	2.86
86.4	4.02	5.32	4.51	3.82	3.24
98.1	4.74	5.97	4.81	3.88	3.49
111	5.21	6.21	4.77	3.71	3.55
127	5.34	5.95	4.39	3.33	3.4
144	5.1	5.24	3.71	2.8	3.07
163	4.54	4.2	2.85	2.21	2.62
186	3.74	3.02	1.96	1.65	2.13
211	2.85	1.88	1.17	1.19	1.67
240	2	0.9	0.46	0.89	1.31
272	1.28	0.3	0.27	0.74	1.07
310	0.72	0.06	0.19	0.72	0.94
352	0.47	0	0.2	0.76	0.89
400	0.36	0	0.21	0.82	0.89
454	0.32	0	0.2	0.83	0.9
516	0.32	0	0.17	0.79	0.87
586	0.31	0	0.12	0.69	0.82
666	0.32	0	0.06	0.56	0.74
756	0.33	0	0.02	0.46	0.61
859	0.35	0	0	0.36	0.5

Table 5: Continued.

976	0.4	0	0	0.26	0.39
1110	0.46	0	0	0.18	0.32
1260	0.5	0	0	0.09	0.28
1430	0.54	0	0	0	0.25
1630	0.57	0	0	0	0.22
1850	0.55	0	0	0	0.18
2100	0.49	0	0	0	0.15
2390	0.39	0	0	0	0.11
2710	0.28	0	0	0	0.08
3080	0.14	0	0	0	0.04
3500	0	0	0	0	0
Size (μm)	260 cm volume %	270 cm volume %	280 cm volume %		
0.01	0	0	0		
0.0114	0	0	0		
0.0129	0	0	0		
0.0147	0	0	0		
0.0167	0	0	0		
0.0189	0	0	0		
0.0215	0	0	0		
0.0244	0	0	0		
0.0278	0	0	0		
0.0315	0	0	0		
0.0358	0	0	0		
0.0407	0	0	0		
0.0463	0	0	0		
0.0526	0	0	0		
0.0597	0	0	0		
0.0679	0	0	0		
0.0771	0	0	0		
0.0876	0	0	0		
0.0995	0	0	0		
0.113	0	0	0		
0.128	0	0	0		
0.146	0	0	0		
0.166	0	0	0		
0.188	0	0	0		
0.214	0	0	0		
0.243	0	0	0		
0.276	0	0	0		
0.314	0.17	0.15	0.2		
0.357	0.35	0.33	0.42		
0.405	0.57	0.52	0.67		
0.46	0.77	0.71	0.91		

Table 5: Continued.

0.523	0.94	0.86	1.1
0.594	1.05	0.96	1.23
0.675	1.11	1.01	1.3
0.767	1.13	1.04	1.34
0.872	1.15	1.06	1.36
0.991	1.19	1.09	1.41
1.13	1.25	1.15	1.49
1.28	1.36	1.23	1.61
1.45	1.51	1.35	1.75
1.65	1.68	1.47	1.92
1.88	1.87	1.6	2.08
2.13	2.03	1.7	2.21
2.42	2.16	1.76	2.3
2.75	2.24	1.78	2.32
3.12	2.26	1.76	2.3
3.55	2.25	1.71	2.24
4.03	2.21	1.65	2.17
4.58	2.16	1.58	2.08
5.21	2.1	1.52	2
5.92	2.03	1.46	1.92
6.72	1.95	1.41	1.86
7.64	1.88	1.37	1.8
8.68	1.81	1.35	1.76
9.86	1.75	1.33	1.72
11.2	1.7	1.33	1.7
12.7	1.64	1.33	1.67
14.5	1.58	1.32	1.65
16.4	1.52	1.3	1.62
18.7	1.46	1.27	1.59
21.2	1.4	1.23	1.57
24.1	1.34	1.18	1.55
27.4	1.29	1.14	1.54
31.1	1.28	1.13	1.55
35.3	1.32	1.17	1.58
40.1	1.44	1.31	1.65
45.6	1.63	1.57	1.77
51.8	1.92	1.96	1.92
58.9	2.28	2.47	2.12
66.9	2.68	3.06	2.34
76	3.07	3.67	2.56
86.4	3.4	4.22	2.73
98.1	3.62	4.64	2.82
111	3.69	4.86	2.81
127	3.6	4.86	2.69
144	3.36	4.62	2.46

Table 5: Continued.

163	3.01	4.17	2.18
186	2.59	3.57	1.88
211	2.12	2.88	1.6
240	1.64	2.15	1.38
272	1.18	1.46	1.21
310	0.73	0.85	1.07
352	0.4	0.28	0.94
400	0.16	0.08	0.8
454	0	0.01	0.62
516	0	0	0.43
586	0	0	0.31
666	0	0	0.18
756	0	0	0.05
859	0	0	0
976	0	0	0
1110	0	0	0
1260	0	0	0
1430	0	0	0
1630	0	0	0
1850	0	0	0
2100	0	0	0
2390	0	0	0
2710	0	0	0
3080	0	0	0
3500	0	0	0

Table 6: Absolute ^{14}C age data used to fit age-D/L models. The ID numbers correspond to unique identification numbers for AAR analyses at Northern Arizona University. Yellow ID specimens are from CB 1-2, blue ID are live-collected specimens, grey ID are specimens collected from Olszewski and Kaufman (2015), and green ID are specimens from CB 2-2.

ID	Asp D/L	Glu D/L	Depth (cm)	^{14}C age	Cal age Yrs BP	Cal BP 1 σ down	Cal BP 1 σ up	Cal BP 2 σ down	Cal BP 2 σ up
13768	0.199	0.077	81	735	409	365	460	311	477
13745	0.366	0.166	53	5825	6272	6228	6306	6190	6359
13927	0.294	0.112	269	3660	3604	3554	3650	3490	3704
13985	0.393	0.226	331	4475	4712	4652	4667	4671	4787
7089A	0.032	0.013	0	0	0	0	0	0	0
7089B	0.033	0.014	0	0	0	0	0	0	0
7089C	0.035	0.014	0	0	0	0	0	0	0
7089D	0.035	0.015	0	0	0	0	0	0	0
7089E	0.034	0.016	0	0	0	0	0	0	0
7089F	0.035	0.015	0	0	0	0	0	0	0
7089G	0.033	0.014	0	0	0	0	0	0	0
7089H	0.034	0.015	0	0	0	0	0	0	0
7089I	0.035	0.015	0	0	0	0	0	0	0
7089J	0.032	0.014	0	0	0	0	0	0	0
UAL8078	0.224	0.086	62	730	403	360	456	309	473
UAL8077	0.167	0.067	61	740	415	375	465	315	480
UAL8105	0.252	0.106	52	830	487	463	510	431	532
UAL8088	0.332	0.146	74	3110	2919	2860	2967	2816	3037
14163	0.166	0.071	27	540	204	146	263	100	287
14201	0.278	0.107	67	1555	1150	1100	1205	1053	1240
14219	0.311	0.135	90	1825	1398	1341	1450	1310	1501
14276	0.373	0.164	170	3820	3808	3749	3867	3689	3912
14334	0.407	0.192	245	5535	5948	5904	5982	5874	6062

Table 7: Core CB 1-2 specimens.

ID	Depth (cm)	Asp D/L	Glu D/L	Asp age	Glu age	Mean age
13712	1	0.054	0.025	4.798080378	92.26639259	48.53223648
13713	2	0.053	0.035	4.594976009	200.8809448	102.7379604
13714	5	0.044	0.020	1.817783432	48.50679618	25.16228981
13715	6	0.050	0.019	3.595302052	38.65636882	21.12583544
13716	7	0.061	0.031	7.764565319	149.3358596	78.55021247
13717	10	0.065	0.034	10.26478525	180.8220021	95.5433937
13718	14	0.396	0.181	5524.179656	4276.269271	4900.224463
13719	15	0.073	0.033	15.12889302	177.4637213	96.29630713
13720	16	0.118	0.064	84.79243486	648.9094304	366.8509326
13721	17	0.079	0.039	20.08843195	242.1229963	131.1057141
13722	19	0.081	0.041	22.60006415	279.9496863	151.2748752
13723	20	0.083	0.038	24.22857197	233.5262409	128.8774064
13724	21	0.088	0.043	30.27680562	308.0011892	169.1389974
13725	23	0.074	0.033	15.86248606	174.6923674	95.27742673
13726	24	0.189	0.081	430.5015694	1002.071528	716.2865489
13727	25	0.185	0.059	400.6440559	562.4899932	481.5670245
13728	26	0.364	0.157	4138.74335	3333.360979	3736.052165
13729	28	0.177	0.055	347.0778827	481.1092231	414.0935529
13730	29	0.233	0.072	886.1178622	810.4136759	848.265769
13731	31	0.220	0.089	729.6802881	1187.072633	958.3764604
13732	33	0.107	0.050	60.6398558	402.2124986	231.4261772
13733	34	0.123	0.058	97.27145825	548.803397	323.0374276
13734	39	0.174	0.081	325.7060598	1014.534931	670.1204955
13735	43	0.168	0.071	289.0590319	791.1388558	540.0989439
13736	44	0.324	0.168	2762.660008	3736.116252	3249.38813
13737	46	0.096	0.047	40.55115262	353.5074222	197.0292874
13738	47	0.161	0.064	247.5835012	646.8308681	447.2071846
13739	48	0.122	0.066	96.21364677	698.4702314	397.3419391
13740	49	0.115	0.050	77.17108217	405.2327034	241.2018928
13741	50	0.203	0.087	550.6737654	1141.685886	846.1798257
13742	51	0.360	0.193	3977.353053	4785.645222	4381.499138
13743	52	0.173	0.072	319.3476433	801.223975	560.2858092
13744	53	0.152	0.073	204.0939271	829.1551134	516.6245203
13745	54	0.366	0.166	4196.902757	3670.671486	3933.787121
13746	55	0.063	0.032	8.79325225	163.1777412	85.98549671
13747	56	0.137	0.067	142.2735026	706.5262699	424.3998862
13748	57	0.149	0.065	191.1833303	674.8058868	432.9946085
13749	58	0.087	0.023	28.68981765	74.11693196	51.4033748
13750	59	0.129	0.044	116.6446687	317.2098132	216.9272409
13751	60	0.375	0.176	4573.726223	4063.948886	4318.837554

Table 7: Continued.

13752	61	0.213	0.088	652.0154283	1181.815568	916.9154981
13753	63	0.179	0.085	358.6762869	1089.816558	724.2464223
13754	64	0.200	0.072	522.9579532	820.6459154	671.8019343
13755	65	0.148	0.064	184.3845527	657.1623621	420.7734574
13756	66	0.120	0.055	90.20748436	492.3307196	291.269102
13757	68	0.124	0.050	101.5194834	403.9267861	252.7231347
13758	69	0.353	0.141	3719.100219	2724.298463	3221.699341
13759	71	0.118	0.050	85.15117183	399.3460125	242.2485922
13760	73	0.122	0.060	95.95485783	576.6368012	336.2958295
13761	74	0.123	0.057	97.29209503	528.2035797	312.7478374
13762	75	0.362	0.150	4064.060157	3073.733586	3568.896872
13763	77	0.211	0.103	627.9518358	1562.308538	1095.130187
13764	78	0.322	0.141	2714.546598	2734.395056	2724.470827
13765	79	0.223	0.100	760.4776735	1467.926135	1114.201904
13766	80	0.080	0.037	21.90733539	225.6448926	123.776114
13767	81	0.152	0.052	201.2541822	439.4443592	320.3492707
13768	82	0.199	0.077	515.5022654	912.2502761	713.8762708
13769	84	0.167	0.065	282.4564924	678.2611856	480.358839
13770	86	0.205	0.097	572.9045192	1390.866449	981.8854839
13771	87	0.162	0.090	253.3356896	1228.686534	741.0111116
13772	88	0.064	0.033	9.302015436	172.6047768	90.95339613
13773	89	0.202	0.081	545.9781055	1007.554575	776.76634
13774	90	0.147	0.078	181.7456051	931.4864226	556.6160139
13775	92	0.114	0.044	74.71265815	323.0207404	198.8666993
13776	93	0.142	0.080	161.2561713	994.4427123	577.8494418
13777	94	0.197	0.077	501.6639316	910.9905744	706.327253
13778	95	0.342	0.173	3344.573266	3921.508754	3633.04101
13779	96	0.182	0.061	378.4522146	588.54765	483.4999323
13780	97	0.137	0.072	143.3890697	803.6291116	473.5090907
13781	98	0.071	0.040	13.832264	259.4980322	136.6651481
13782	99	0.231	0.095	865.7564418	1359.5428	1112.649621
13783	100	0.175	0.065	330.8701354	680.0007472	505.4354413
13784	101	0.383	0.193	4929.653304	4773.367626	4851.510465
13785	102	0.159	0.047	238.4340079	362.8233854	300.6286966
13786	103	0.132	0.028	126.260549	118.1036486	122.1820988
13787	104	0.326	0.106	2832.924126	1631.855672	2232.389899
13788	105	0.150	0.051	192.359688	430.0788419	311.2192649
13789	107	0.173	0.062	315.9603492	618.3422233	467.1512862
13790	109	0.216	0.082	687.8140069	1037.345968	862.5799875
13791	110	0.311	0.122	2404.553952	2127.351977	2265.952965
13792	111	0.337	0.145	3168.623342	2888.34575	3028.484546
13793	112	0.230	0.106	849.4410195	1629.630121	1239.53557

Table 7: Continued.

13794	113	0.192	0.076	459.5183268	901.3774689	680.4478978
13795	115	0.341	0.116	3293.458416	1920.607294	2607.032855
13796	116	0.156	0.052	224.2113517	439.5148835	331.8631176
13797	117	0.354	0.148	3765.609871	2992.029594	3378.819732
13798	118	0.142	0.052	161.4943335	435.9092673	298.7018004
13799	119	0.223	0.095	769.339686	1359.30548	1064.322583
13800	120	0.198	0.071	509.7537901	780.4544798	645.104135
13801	122	0.100	0.036	47.51938225	204.0981775	125.8087799
13802	126	0.166	0.066	278.4117084	693.5294248	485.9705666
13803	127	0.154	0.091	211.6290646	1253.634524	732.6317942
13804	128	0.332	0.125	3007.541525	2203.747856	2605.64469
13805	131	0.105	0.055	56.92708585	480.8537028	268.8903943
13806	132	0.354	0.182	3743.375203	4304.757296	4024.066249
13807	133	0.379	0.193	4760.548453	4785.3535	4772.950977
13808	136	0.311	0.137	2414.713614	2604.413433	2509.563523
13809	137	0.338	0.156	3205.121272	3289.99091	3247.556091
13810	138	0.358	0.180	3892.651789	4232.729523	4062.690656
13811	139	0.135	0.041	135.30196	271.8310918	203.5665259
13812	140	0.119	0.042	87.08129543	285.7363208	186.4088081
13813	141	0.364	0.162	4144.410697	3512.141951	3828.276324
13814	145	0.195	0.085	482.1281594	1090.24898	786.1885696
13815	146	0.283	0.119	1730.801604	2012.654661	1871.728133
13816	147	0.276	0.109	1595.963353	1717.476787	1656.72007
13817	148	0.122	0.037	96.14388455	225.1023064	160.6230955
13818	150	0.218	0.089	706.7668506	1205.849806	956.3083281
13819	151	0.344	0.131	3401.694494	2389.129402	2895.411948
13820	152	0.244	0.081	1038.060241	1006.554831	1022.307536
13821	154	0.398	0.207	5607.530282	5430.324653	5518.927468
13822	155	0.354	0.175	3742.724372	4017.364463	3880.044417
13823	156	0.295	0.132	1990.763203	2425.215515	2207.989359
13824	157	0.311	0.148	2396.61846	2990.588377	2693.603418
13825	158	0.364	0.183	4138.618961	4362.897995	4250.758478
13826	159	0.390	0.194	5230.296126	4840.666761	5035.481443
13827	160	0.365	0.191	4184.680104	4691.341532	4438.010818
13828	161	0.335	0.140	3098.787653	2702.117313	2900.452483
13829	162	0.340	0.145	3265.506208	2868.847911	3067.17706
13830	163	0.237	0.080	945.3111562	978.2156538	961.763405
13831	164	0.143	0.059	165.8492619	564.5811998	365.2152309
13832	165	0.352	0.158	3673.509509	3338.983909	3506.246709
13833	166	0.254	0.106	1197.535633	1655.409094	1426.472363
13834	167	0.375	0.175	4563.800443	4011.823806	4287.812125
13835	169	0.355	0.161	3770.272034	3463.153668	3616.712851

Table 7: Continued.

13836	170	0.377	0.178	4649.028032	4131.174496	4390.101264
13837	171	0.347	0.182	3510.445247	4308.334922	3909.390085
13838	172	0.331	0.133	2971.388524	2455.399192	2713.393858
13839	173	0.219	0.044	716.8395339	318.8174536	517.8284938
13840	175	0.105	0.014	56.5965415	4.829734277	30.71313789
13841	176	0.325	0.157	2786.717361	3318.954843	3052.836102
13842	178	0.352	0.156	3663.376203	3259.687322	3461.531763
13843	179	0.348	0.169	3528.883062	3787.497977	3658.190519
13844	181	0.360	0.168	3972.008397	3750.591871	3861.300134
13845	182	0.244	0.087	1040.504106	1150.662562	1095.583334
13846	183	0.387	0.188	5090.994123	4547.579823	4819.286973
13847	185	0.318	0.161	2587.70113	3450.213698	3018.957414
13848	189	0.334	0.154	3084.76042	3190.281141	3137.520781
13849	190	0.339	0.128	3226.140521	2313.426713	2769.783617
13850	191	0.240	0.114	977.2051514	1860.758799	1418.981975
13851	192	0.303	0.089	2186.020152	1202.257236	1694.138694
13852	193	0.348	0.097	3541.297935	1402.249775	2471.773855
13853	194	0.343	0.184	3359.122805	4388.039439	3873.581122
13854	195	0.327	0.170	2852.792276	3824.569367	3338.680822
13855	196	0.080	0.033	21.09001813	170.2515093	95.67076371
13856	197	0.356	0.176	3837.726958	4045.641375	3941.684166
13857	198	0.355	0.189	3794.412342	4610.770723	4202.591532
13858	199	0.304	0.096	2230.75744	1367.617553	1799.187497
13859	200	0.343	0.180	3355.95777	4220.901669	3788.429719
13860	201	0.338	0.167	3199.112612	3718.055261	3458.583936
13861	202	0.365	0.186	4169.887865	4478.585727	4324.236796
13862	203	0.334	0.136	3057.13252	2566.257258	2811.694889
13863	204	0.344	0.150	3402.528618	3046.367693	3224.448156
13864	205	0.322	0.135	2694.405052	2549.178221	2621.791636
13865	206	0.323	0.148	2727.84239	2969.744624	2848.793507
13866	207	0.351	0.172	3652.862472	3893.833931	3773.348202
13867	208	0.322	0.150	2702.536999	3063.859101	2883.19805
13868	209	0.316	0.124	2536.497864	2189.636465	2363.067164
13869	210	0.387	0.153	5076.69963	3148.355064	4112.527347
13870	211	0.373	0.193	4478.661941	4798.125028	4638.393485
13871	212	0.319	0.165	2612.092489	3602.745075	3107.418782
13872	213	0.347	0.157	3493.983848	3313.347627	3403.665738
13873	214	0.343	0.164	3378.038362	3589.323079	3483.680721
13874	215	0.331	0.153	2966.802045	3150.066942	3058.434493
13875	216	0.335	0.166	3096.524169	3663.183684	3379.853927
13876	217	0.337	0.171	3165.710094	3852.172626	3508.94136
13877	218	0.347	0.157	3518.165628	3296.530053	3407.347841

Table 7: Continued.

13878	219	0.336	0.167	3129.114526	3707.292363	3418.203444
13879	220	0.297	0.157	2054.957446	3314.840411	2684.898929
13880	221	0.195	0.042	481.2430914	284.508333	382.8757122
13881	222	0.333	0.137	3051.720306	2603.837913	2827.77911
13882	223	0.307	0.145	2302.606993	2860.347672	2581.477333
13883	224	0.364	0.174	4127.887943	3982.738462	4055.313203
13884	225	0.412	0.217	6315.26503	5878.564838	6096.914934
13885	226	0.377	0.182	4667.550347	4322.951861	4495.251104
13886	227	0.336	0.199	3136.269592	5061.892253	4099.080923
13887	228	0.328	0.146	2870.279707	2897.537679	2883.908693
13888	229	0.370	0.212	4388.203644	5644.607253	5016.405449
13889	230	0.340	0.159	3255.88798	3376.098837	3315.993408
13890	231	0.363	0.168	4080.246591	3726.54055	3903.39357
13891	232	0.353	0.174	3701.201944	3962.347686	3831.774815
13892	233	0.355	0.147	3777.910775	2934.325322	3356.118048
13893	234	0.355	0.178	3784.611168	4131.835973	3958.22357
13894	235	0.341	0.163	3290.879544	3534.78661	3412.833077
13895	236	0.381	0.220	4853.556335	6034.206285	5443.88131
13896	237	0.338	0.159	3215.397533	3395.578582	3305.488057
13897	238	0.330	0.137	2952.503997	2600.991182	2776.747589
13898	239	0.298	0.152	2072.421637	3118.436252	2595.428945
13899	240	0.352	0.160	3678.563433	3426.824897	3552.694165
13900	241	0.309	0.148	2336.25084	2980.437019	2658.343929
13901	242	0.331	0.156	2970.497819	3262.315713	3116.406766
13902	243	0.307	0.145	2302.606993	2860.347672	2581.477333
13904	245	0.342	0.139	3332.529561	2666.91979	2999.724675
13905	246	0.315	0.144	2522.132915	2840.401003	2681.266959
13906	248	0.326	0.147	2826.243223	2966.176709	2896.209966
13907	249	0.385	0.168	5021.828037	3739.045944	4380.43699
13908	251	0.344	0.177	3414.978026	4094.517896	3754.747961
13909	252	0.338	0.131	3198.286656	2416.506398	2807.396527
13910	253	0.370	0.148	4388.58302	2980.051721	3684.31737
13911	254	0.326	0.225	2831.597101	6246.925429	4539.261265
13912	255	0.347	0.144	3514.689895	2843.559133	3179.124514
13913	256	0.324	0.154	2752.591832	3200.01062	2976.301226
13914	257	0.311	0.143	2396.568129	2799.293413	2597.930771
13915	258	0.333	0.120	3038.654331	2061.748854	2550.201592
13916	259	0.336	0.125	3128.806059	2217.876459	2673.341259
13917	260	0.326	0.132	2837.114849	2437.8144	2637.464625
13918	261	0.335	0.123	3087.984726	2129.686265	2608.835496
13919	262	0.322	0.175	2698.101218	4007.247007	3352.674113
13920	263	0.342	0.175	3326.127458	4021.321499	3673.724478

Table 7: Continued.

13921	264	0.345	0.152	3424.654569	3112.017049	3268.335809
13922	265	0.321	0.148	2692.026401	2983.53193	2837.779166
13923	266	0.347	0.187	3498.527604	4523.505265	4011.016434
13924	267	0.327	0.139	2840.962334	2677.285004	2759.123669
13925	268	0.335	0.139	3103.337141	2671.485165	2887.411153
13926	269	0.346	0.129	3478.882243	2338.790323	2908.836283
13927	270	0.294	0.112	1982.049832	1808.413309	1895.23157
13928	271	0.404	0.220	5911.397574	6049.043737	5980.220656
13929	272	0.332	0.146	2997.397985	2919.80299	2958.600487
13930	273	0.315	0.130	2498.078265	2374.860354	2436.46931
13931	274	0.358	0.175	3900.839864	4000.871075	3950.85547
13932	275	0.385	0.188	5026.950541	4571.281851	4799.116196
13933	276	0.350	0.163	3621.029855	3556.756927	3588.893391
13934	277	0.344	0.163	3398.433923	3543.43873	3470.936327
13935	278	0.333	0.129	3052.187265	2324.508123	2688.347694
13936	279	0.354	0.159	3745.545897	3406.81495	3576.180424
13937	280	0.364	0.127	4122.735047	2287.010444	3204.872746
13938	281	0.356	0.188	3832.770115	4569.884549	4201.327332
13939	282	0.358	0.173	3889.198557	3927.695291	3908.446924
13940	283	0.396	0.197	5502.467479	4958.569989	5230.518734
13941	284	0.387	0.177	5091.546574	4109.436886	4600.49173
13942	285	0.355	0.161	3794.937578	3477.570453	3636.254016
13943	286	0.361	0.171	3997.008334	3870.327644	3933.667989
13944	287	0.323	0.137	2742.886726	2609.877313	2676.382019
13945	288	0.375	0.203	4585.900543	5225.626474	4905.763508
13946	289	0.354	0.198	3733.71668	4987.463383	4360.590032
13947	290	0.361	0.121	4015.825241	2073.363788	3044.594514
13948	291	0.387	0.187	5088.281131	4532.846259	4810.563695
13949	292	0.353	0.173	3699.706145	3918.53872	3809.122432
13950	293	0.359	0.190	3925.481455	4647.635555	4286.558505
13951	294	0.338	0.161	3209.506683	3478.629667	3344.068175
13952	295	0.380	0.183	4778.335772	4352.781681	4565.558726
13953	298	0.341	0.116	3301.890265	1938.157001	2620.023633
13954	299	0.368	0.178	4272.606458	4127.780279	4200.193368
13955	300	0.394	0.199	5427.650436	5025.582451	5226.616444
13956	301	0.379	0.179	4762.461742	4193.292005	4477.876873
13957	302	0.365	0.150	4152.538181	3064.36452	3608.45135
13958	303	0.374	0.159	4536.458115	3388.228825	3962.34347
13959	304	0.385	0.227	5022.58737	6372.963786	5697.775578
13960	305	0.361	0.155	4025.66375	3256.49173	3641.07774
13961	306	0.421	0.223	6808.444981	6194.800848	6501.622914
13962	307	0.292	0.122	1927.763103	2123.539002	2025.651052

Table 7: Continued.

13963	308	0.362	0.174	4061.63894	3983.881343	4022.760141
13964	309	0.342	0.166	3342.769605	3672.397334	3507.583469
13965	310	0.346	0.160	3451.639799	3414.225235	3432.932517
13966	311	0.363	0.155	4095.375177	3230.52636	3662.950769
13967	312	0.341	0.157	3312.517142	3308.745474	3310.631308
13968	314	0.348	0.163	3533.803175	3560.5348	3547.168988
13969	315	0.362	0.186	4038.813356	4488.263106	4263.538231
13970	316	0.350	0.157	3611.286531	3328.42183	3469.85418
13971	317	0.374	0.174	4526.210779	3996.633248	4261.422013
13972	318	0.362	0.173	4038.539266	3952.043589	3995.291427
13973	319	0.391	0.198	5266.100864	5016.168855	5141.13486
13974	321	0.379	0.179	4763.50466	4174.778259	4469.141459
13975	322	0.387	0.187	5088.281131	4532.846259	4810.563695
13976	323	0.380	0.215	4806.84882	5790.643265	5298.746042
13977	324	0.356	0.182	3817.103619	4309.293964	4063.198791
13978	325	0.369	0.188	4332.743674	4544.315972	4438.529823
13979	326	0.336	0.175	3128.179264	4004.373381	3566.276323
13980	327	0.434	0.152	7588.279162	3121.081577	5354.68037
13981	328	0.391	0.215	5260.736103	5780.967786	5520.851944
13982	329	0.386	0.168	5057.816748	3748.596425	4403.206586
13983	330	0.369	0.188	4339.393557	4549.609303	4444.50143
13984	331	0.386	0.156	5049.163141	3279.634794	4164.398968
13985	332	0.393	0.226	5394.614918	6332.849477	5863.732197
13986	333	0.429	0.218	7287.173756	5906.416359	6596.795058
13987	334	0.337	0.157	3178.402386	3304.287258	3241.344822
13988	335	0.352	0.164	3692.251581	3587.65317	3639.952375
13989	336	0.370	0.189	4381.876614	4626.803675	4504.340144
13990	337	0.365	0.181	4155.807867	4282.082554	4218.94521
13991	338	0.370	0.116	4375.323693	1935.047575	3155.185634
13992	339	0.383	0.177	4912.80772	4119.519138	4516.163429
13993	340	0.364	0.154	4133.804701	3191.813387	3662.809044
13994	342	0.331	0.160	2969.851143	3440.388582	3205.119863
13995	343	0.349	0.135	3571.496053	2541.73627	3056.616162
13996	344	0.384	0.190	4965.15328	4635.136418	4800.144849
13997	345	0.351	0.150	3650.385499	3051.749087	3351.067293
13998	346	0.358	0.155	3896.621999	3230.323565	3563.472782
13999	347	0.376	0.196	4633.675526	4908.297461	4770.986493
14000	348	0.376	0.166	4620.097171	3647.504046	4133.800609
14001	349	0.393	0.213	5385.429188	5711.479338	5548.454263
14002	351	0.359	0.166	3927.959945	3679.165904	3803.562924
14003	354	0.348	0.134	3551.110445	2485.984895	3018.54767
14004	355	0.345	0.159	3422.311176	3377.624205	3399.967691

Table 7: Continued.

14005	356	0.353	0.106	3715.172555	1652.544024	2683.85829
13903B	244	0.319	0.119	2609.003208	2012.929515	2310.966362

Table 8: Core CB 2-2 specimens

ID	Depth (cm)	Asp D/L	Glu D/L	Asp age	Glu age	Mean age
14156	20	0.176	0.091	337.8154636	1251.604673	794.7100682
14157	21	0.167	0.072	281.8448961	811.1097535	546.4773248
14158	22	0.176	0.070	340.6473817	778.2343975	559.4408896
14159	23	0.159	0.068	236.674974	729.1518842	482.9134291
14160	24	0.176	0.087	339.4211732	1149.540252	744.4807128
14161	25	0.158	0.060	230.1980717	581.7324432	405.9652574
14162	26	0.146	0.073	176.5214485	833.5313885	505.0264185
14163	27	0.166	0.071	276.7118075	788.9990422	532.8554248
14164	28	0.164	0.063	265.4098418	624.258364	444.8341029
14165	29	0.157	0.069	225.1850129	741.7619822	483.4734976
14166	30	0.224	0.094	775.2194694	1326.314257	1050.766863
14167	31	0.211	0.087	631.3130138	1155.56525	893.4391319
14168	32	0.196	0.071	493.2051541	798.7610481	645.9831011
14169	33	0.199	0.086	519.3297053	1117.60322	818.4664624
14170	34	0.173	0.069	317.7723698	743.5317907	530.6520803
14171	36	0.177	0.065	346.7357123	672.3577842	509.5467483
14172	38	0.207	0.086	592.3470315	1135.562934	863.9549827
14173	39	0.193	0.091	466.0436271	1252.805215	859.424421
14174	40	0.219	0.081	711.6884747	1003.813419	857.7509469
14175	41	0.356	0.155	3838.802824	3227.852261	3533.327543
14176	42	0.179	0.078	360.5602674	944.7767316	652.6684995
14177	43	0.177	0.080	344.0917971	983.6803181	663.8860576
14178	44	0.214	0.091	664.6150803	1258.468306	961.5416933
14179	45	0.192	0.072	452.0476818	820.6448337	636.3462578
14180	46	0.203	0.080	552.5034624	980.9329778	766.7182201
14181	47	0.188	0.081	420.0587931	1017.157517	718.6081549
14182	48	0.242	0.122	1008.901871	2109.669272	1559.285572
14183	49	0.212	0.098	638.0791505	1436.7008	1037.389975
14184	50	0.220	0.090	733.0180082	1229.241079	981.1295436

Table 8: Continued.

14185	51	0.217	0.099	690.0631502	1448.403101	1069.233126
14186	52	0.214	0.083	662.0423217	1048.536885	855.2896033
14187	53	0.344	0.156	3411.157607	3290.095514	3350.626561
14188	54	0.273	0.097	1534.42679	1391.413221	1462.920006
14189	55	0.266	0.111	1405.927258	1771.7367	1588.831979
14190	56	0.215	0.092	675.5997393	1264.216169	969.907954
14191	57	0.291	0.139	1901.369204	2660.056924	2280.713064
14192	58	0.256	0.101	1233.860367	1494.779818	1364.320092
14193	59	0.320	0.156	2655.805004	3267.721168	2961.763086
14194	60	0.270	0.107	1479.501651	1658.454125	1568.977888
14195	61	0.270	0.138	1479.651395	2640.611503	2060.131449
14196	62	0.349	0.148	3554.706655	3001.014083	3277.860369
14197	63	0.296	0.122	2017.978724	2109.963681	2063.971203
14198	64	0.306	0.126	2279.828304	2241.475371	2260.651837
14199	65	0.269	0.115	1455.893017	1912.445151	1684.169084
14200	66	0.279	0.109	1646.278398	1714.263196	1680.270797
14201	67	0.278	0.107	1627.401537	1669.869258	1648.635397
14202	68	0.275	0.121	1572.390944	2097.575135	1834.983039
14203	69	0.272	0.103	1513.454595	1566.179374	1539.816985
14204	70	0.269	0.124	1457.251301	2164.863136	1811.057218
14205	71	0.296	0.135	2033.780815	2539.373997	2286.577406
14206	72	0.308	0.151	2320.973016	3096.642006	2708.807511
14207	73	0.300	0.143	2113.884769	2796.400134	2455.142452
14208	74	0.363	0.164	4082.128165	3577.372754	3829.75046
14209	75	0.296	0.129	2014.436869	2346.263229	2180.350049
14210	76	0.299	0.127	2104.402937	2268.781689	2186.592313
14211	78	0.301	0.117	2141.209954	1958.119954	2049.664954
14212	80	0.358	0.156	3903.874887	3278.333916	3591.104401
14213	83	0.302	0.148	2174.351883	2975.496709	2574.924296
14214	84	0.331	0.128	2973.034357	2300.817257	2636.925807
14215	85	0.343	0.158	3368.186473	3354.663216	3361.424845
14216	87	0.289	0.123	1864.920676	2151.391498	2008.156087
14217	88	0.340	0.154	3254.732476	3199.429454	3227.080965
14218	89	0.319	0.143	2613.179773	2820.915737	2717.047755
14219	90	0.311	0.135	2390.342673	2541.91677	2466.129721
14220	92	0.324	0.134	2778.565427	2483.556338	2631.060883
14221	93	0.293	0.113	1950.488807	1843.302191	1896.895499
14222	94	0.313	0.129	2451.858407	2340.190994	2396.0247

Table 8: Continued.

14223	95	0.332	0.135	2992.349135	2538.884216	2765.616675
14224	96	0.324	0.136	2754.542324	2569.75318	2662.147752
14225	97	0.308	0.147	2330.837243	2942.573208	2636.705226
14226	98	0.313	0.125	2467.753166	2204.284548	2336.018857
14227	99	0.324	0.165	2760.953991	3639.976029	3200.46501
14228	100	0.334	0.158	3064.136419	3357.222223	3210.679321
14229	101	0.301	0.142	2156.462851	2770.485837	2463.474344
14230	102	0.372	0.177	4455.291104	4096.94088	4276.115992
14231	103	0.349	0.174	3555.992702	3981.636631	3768.814666
14232	104	0.335	0.151	3103.324123	3093.021423	3098.172773
14233	105	0.357	0.191	3844.277067	4704.399986	4274.338527
14234	106	0.336	0.174	3148.149225	3979.120562	3563.634894
14235	110	0.372	0.199	4467.462783	5041.594638	4754.52871
14236	111	0.313	0.127	2442.555754	2275.883634	2359.219694
14237	112	0.357	0.202	3866.886394	5190.027546	4528.45697
14238	113	0.319	0.158	2620.233334	3342.85615	2981.544742
14239	114	0.338	0.130	3190.688238	2363.271194	2776.979716
14240	115	0.323	0.128	2737.441168	2293.014654	2515.227911
14241	116	0.408	0.254	6107.548244	7746.1962	6926.872222
14242	117	0.309	0.131	2354.595199	2416.247988	2385.421594
14243	118	0.338	0.125	3188.351706	2210.515459	2699.433582
14244	119	0.356	0.165	3835.020566	3616.856939	3725.938752
14245	120	0.340	0.168	3251.049956	3730.43939	3490.744673
14246	121	0.389	0.188	5173.024332	4572.135434	4872.579883
14247	122	0.312	0.145	2440.851198	2873.786356	2657.318777
14248	124	0.351	0.182	3653.709177	4302.269367	3977.989272
14249	126	0.367	0.168	4253.838392	3733.01643	3993.427411
14250	128	0.343	0.138	3380.079462	2629.930779	3005.005121
14251	130	0.385	0.192	5024.698047	4724.867407	4874.782727
14252-						
1	131	0.352	0.164	3682.596064	3591.28475	3636.940407
14252-						
2	131	0.355	0.166	3797.772134	3655.524629	3726.648381
14253	134	0.269	0.101	1449.131994	1500.664364	1474.898179
14254	136	0.390	0.130	5256.512053	2356.853947	3806.683
14255	139	0.324	0.172	2758.300753	3897.35436	3327.827557
14256	143	0.353	0.157	3714.306524	3326.358338	3520.332431
14257	146	0.364	0.170	4113.218629	3824.513745	3968.866187

Table 8: Continued.

14258	147	0.286	0.187	1806.040173	4540.425944	3173.233058
14259	148	0.341	0.178	3290.314915	4144.456722	3717.385819
14260	149	0.373	0.214	4508.483052	5735.247554	5121.865303
14261	150	0.361	0.168	4019.246534	3721.709627	3870.478081
14262	151	0.321	0.161	2666.824419	3470.768934	3068.796677
14263	152	0.369	0.158	4334.557212	3356.392347	3845.47478
14264	153	0.346	0.194	3451.342864	4805.606503	4128.474684
14265	154	0.352	0.164	3667.22584	3593.360632	3630.293236
14266	155	0.278	0.120	1640.413731	2057.223846	1848.818788
14267	156	0.357	0.147	3855.431519	2954.641153	3405.036336
14268	157	0.367	0.184	4247.044478	4389.270793	4318.157636
14269	158	0.305	0.118	2238.716785	1989.011692	2113.864238
14270-						
1	161	0.424	0.184	6979.767789	4381.73678	5680.752285
14270-						
2	161	0.407	0.185	6085.481711	4430.041157	5257.761434
14271	162	0.348	0.187	3550.247162	4516.828098	4033.53763
14272	163	0.376	0.202	4620.553108	5193.797259	4907.175184
14273	165	0.305	0.145	2236.077372	2861.774224	2548.925798
14274	166	0.349	0.189	3565.876545	4596.088515	4080.98253
14275	168	0.338	0.146	3185.466172	2914.445137	3049.955654
14276	170	0.373	0.164	4475.822413	3579.733255	4027.777834
14277	171	0.366	0.142	4223.830671	2780.929026	3502.379848
14278	174	0.335	0.152	3096.978888	3139.123496	3118.051192
14279	175	0.376	0.144	4610.907277	2826.015552	3718.461415
14280	176	0.357	0.156	3879.500736	3275.168095	3577.334415
14281	177	0.365	0.143	4174.910971	2808.634928	3491.772949
14282	178	0.362	0.155	4040.481544	3233.328989	3636.905266
14283	180	0.314	0.149	2487.32917	3014.431634	2750.880402
14284	181	0.339	0.177	3227.755866	4099.177583	3663.466724
14285	182	0.382	0.158	4863.536669	3366.143761	4114.840215
14286	183	0.324	0.145	2773.551048	2877.154303	2825.352675
14287	184	0.362	0.172	4070.163724	3887.942058	3979.052891
14288	185	0.386	0.147	5040.815709	2964.741539	4002.778624
14289	186	0.353	0.156	3731.443022	3271.042632	3501.242827
14290	187	0.387	0.205	5077.180954	5317.804931	5197.492943
14291	190	0.400	0.190	5732.44177	4669.187107	5200.814439
14292	191	0.380	0.138	4781.29785	2621.516833	3701.407341
14293	192	0.387	0.189	5088.932867	4620.910297	4854.921582

Table 8: Continued.

14294	193	0.374	0.198	4541.603638	4986.061919	4763.832778
14295	194	0.385	0.174	5013.160829	3997.782034	4505.471431
14296	195	0.390	0.216	5243.963169	5828.760953	5536.362061
14297	197	0.351	0.145	3649.138127	2872.915892	3261.027009
14298	198	0.349	0.172	3563.721196	3884.432922	3724.077059
14299	199	0.370	0.180	4363.224798	4211.908016	4287.566407
14300	200	0.398	0.201	5611.439942	5134.496712	5372.968327
14301	201	0.387	0.216	5116.930693	5835.773045	5476.351869
14302	202	0.404	0.139	5917.174834	2671.665591	4294.420213
14303	203	0.357	0.185	3849.568743	4451.540461	4150.554602
14304	204	0.345	0.152	3433.775987	3130.09279	3281.934389
14305	205	0.342	0.193	3334.327954	4770.824616	4052.576285
14306	207	0.290	0.155	1892.58977	3230.352517	2561.471144
14307	208	0.404	0.185	5893.421705	4440.023165	5166.722435
14308	209	0.359	0.171	3923.809594	3856.257139	3890.033366
14309-	1	0.360	0.169	3975.998467	3777.992459	3876.995463
14309-	2	0.368	0.172	4290.36321	3893.606375	4091.984793
14310	212	0.321	0.084	2686.689875	1069.296455	1877.993165
14311	213	0.369	0.198	4325.117778	5019.894009	4672.505894
14312	214	0.362	0.166	4061.663277	3674.560848	3868.112062
14313	215	0.370	0.200	4359.804289	5106.383616	4733.093953
14314	216	0.320	0.173	2649.249761	3921.318691	3285.284226
14315	217	0.311	0.135	2414.650991	2525.043237	2469.847114
14316	218	0.395	0.227	5471.090673	6349.597482	5910.344078
14317	220	0.321	0.180	2691.071745	4215.837003	3453.454374
14318	222	0.344	0.154	3414.493463	3218.860168	3316.676816
14319	223	0.367	0.228	4248.893316	6413.405411	5331.149364
14320	227	0.396	0.213	5506.5811	5682.099345	5594.340222
14321	228	0.352	0.168	3692.105988	3719.450188	3705.778088
14322	229	0.422	0.213	6896.5966	5709.3996	6302.9981
14323	230	0.382	0.167	4873.086767	3681.802698	4277.444733
14324	232	0.392	0.189	5347.916586	4600.81303	4974.364808
14325	233	0.318	0.158	2592.560847	3350.595649	2971.578248
14326	234	0.377	0.155	4657.524517	3255.714679	3956.619598
14327	236	0.393	0.199	5373.800868	5032.357858	5203.079363
14328	237	0.375	0.197	4584.389991	4943.588749	4763.98937

Table 8: Continued.

14329	238	0.401	0.220	5766.927369	6009.286307	5888.106838
14330	240	0.382	0.178	4888.00763	4154.491749	4521.24969
14331	241	0.438	0.216	7836.075747	5840.066695	6838.071221
14332	243	0.365	0.158	4179.858793	3368.885734	3774.372263
14333	244	0.329	0.156	2902.412227	3275.204464	3088.808346
14334	245	0.407	0.192	6049.650276	4746.438073	5398.044174
14335	246	0.385	0.164	4998.431487	3588.414548	4293.423018
14336	247	0.382	0.134	4877.393879	2492.826879	3685.110379
14337	248	0.402	0.213	5787.962702	5702.887822	5745.425262
14338	249	0.350	0.147	3589.875155	2958.138481	3274.006818
14339	250	0.342	0.177	3328.585502	4097.152145	3712.868823
14340	252	0.406	0.194	6031.359084	4829.935588	5430.647336
14341	253	0.435	0.250	7598.855148	7529.379674	7564.117411
14342	254	0.348	0.234	3522.534108	6740.933754	5131.733931
14343	256	0.406	0.221	6004.136927	6051.34321	6027.740069
14344	258	0.364	0.193	4114.215179	4761.678055	4437.946617
14345	259	0.278	0.125	1637.828533	2221.155576	1929.492055
14346	260	0.378	0.205	4700.982381	5298.538918	4999.76065
14347	262	0.390	0.203	5258.902774	5242.87104	5250.886907
14348	263	0.391	0.187	5289.481068	4503.238634	4896.359851
14349	265	0.421	0.204	6822.587695	5265.590562	6044.089129
14350	266	0.373	0.168	4503.296781	3727.788207	4115.542494
14351	267	0.386	0.199	5042.096	5027.450412	5034.773206
14352-1	269	0.397	0.229	5553.773574	6462.11886	6007.946217
14352-2	269	0.392	0.226	5310.060059	6296.751689	5803.405874
14353	271	0.393	0.149	5396.59034	3014.683797	4205.637068
14354	274	0.395	0.206	5448.59876	5356.106192	5402.352476
14355	275	0.540	0.229	16040.13957	6463.053568	11251.59657
14356	277	0.395	0.186	5471.832618	4488.864531	4980.348575
14357	278	0.380	0.178	4790.400742	4156.419908	4473.410325
14358	279	0.372	0.177	4452.194237	4082.130117	4267.162177
14359-1	283	0.397	0.174	5581.756409	3970.707562	4776.231986
14359-2	283	0.390	0.177	5252.981881	4082.614008	4667.797945

Table 9: CB 1-2 surface specimens.

ID	Core	Asp D/L	Glu D/L	Asp age	Glu age	Mean age
14006A	1-2	0.049	0.027	3.152852067	106.4358974	54.79437474
14006B	1-2	0.053	0.025	4.33747915	91.85086114	48.09417014
14006C	1-2	0.046	0.032	2.435434921	165.6056355	84.0205352
14006D	1-2	0.318	0.144	2601.8157	2859.300442	2730.558071
14006E	1-2	0.043	0.021	1.635035101	57.04515648	29.34009579
14006F	1-2	0.041	0.026	1.342618463	94.28658545	47.81460196
14006G	1-2	0.091	0.052	34.28857884	437.8393241	236.0639515
14006H	1-2	0.047	0.028	2.599118578	121.2386757	61.91889713
14006I	1-2	0.049	0.030	3.218431405	136.0802504	69.6493409
14006J	1-2	0.047	0.022	2.645685791	63.87140492	33.25854536
14006K	1-2	0.039	0.021	0.976372962	54.72087713	27.84862505
14006L	1-2	0.053	0.028	4.622257956	117.6081031	61.11518051
14006M	1-2	0.058	0.044	6.324843139	322.8577429	164.591293
14006N	1-2	0.054	0.028	4.745095935	121.8288082	63.28695207
14006O	1-2	0.046	0.031	2.48375307	148.4823987	75.48307591
14006P	1-2	0.050	0.025	3.498974872	92.80657002	48.15277245
14006Q	1-2	0.045	0.024	2.167341228	82.60553935	42.38644029
14006R	1-2	0.052	0.029	4.194235599	133.5247402	68.85948791
14006S	1-2	0.051	0.029	3.892522375	124.2418872	64.06720481
14006T	1-2	0.355	0.169	3769.863898	3781.380221	3775.622059
14006U	1-2	0.049	0.023	3.203828787	72.8676422	38.03573549
14006V	1-2	0.055	0.029	5.268557665	130.8149068	68.04173222
14006W	1-2	0.056	0.027	5.440107705	110.0357122	57.73790996
14006X	1-2	0.046	0.028	2.259567739	119.9520816	61.10582468
14006Y	1-2	0.049	0.028	3.279889978	120.1389357	61.70941284
14006Z	1-2	0.053	0.024	4.309582296	79.17745647	41.74351938
14006A						
A	1-2	0.045	0.023	2.122883489	73.83309883	37.97799116
14006A						
B	1-2	0.054	0.027	4.826828893	110.1355276	57.48117827
14006A						
C	1-2	0.054 0.0604564	0.027 0.030063	4.820225478	110.8622634	57.84124445
14007A	1-2	17 0.0624373	841 0.034163	7.585511501	140.4326637	74.00908759
14007C	1-2	33 0.0394986	119 0.029392	8.58846149	186.9258249	97.75714318
14007D	1-2	76 0.0405190	152 0.022449	1.015551753	133.2443402	67.12994596
14007E	1-2	25	735	1.196643837	66.27807744	33.73736064
14007F	1-2	0.0429956	0.022997	1.684826807	71.0625586	36.3736927

Table 9: Continued.

		82	205			
		0.0434259	0.023147			
14007G	1-2	82	272	1.776993168	72.38918337	37.08308827
		0.0446141	0.025653			
14007H	1-2	09	029	2.043304175	95.49341443	48.7683593
		0.0514427	0.030288			
14007I	1-2	04	227	3.942460773	142.8612544	73.40185761
		0.0428485	0.030046			
14007J	1-2	02	152	1.653814775	140.2417942	70.9478045
		0.0447755	0.027846			
14007K	1-2	05	926	2.080845842	117.1749342	59.62789004
		0.0707726	0.043652			
14007L	1-2	14	383	13.73821791	311.2666461	162.502432
		0.0420725	0.021929			
14007M	1-2	43	825	1.49456811	61.8151484	31.65485826
		0.0432283	0.023098			
14007N	1-2	23	31	1.734377889	71.95563516	36.84500653
		0.0418677	0.028798			
14007O	1-2	08	268	1.453708908	126.9909464	64.22232764
		0.0510199	0.031639			
14007P	1-2	58	29	3.805207932	157.7708924	80.78805017
		0.0539366	0.041769			
14007Q	1-2	22	717	4.809905885	284.7884628	144.7991843
		0.0551577	0.038335			
14007R	1-2	78	383	5.272052804	238.7739268	122.0229898
		0.0640795	0.045883			
14007S	1-2	25	181	9.481028582	343.773434	176.6272313
		0.0417665	0.022874			
14007T	1-2	02	307	1.433700305	69.98095615	35.70732823
		0.0415623	0.021595			
14007U	1-2	58	9	1.393699603	58.99040513	30.19205237
		0.0395348	0.021639			
14007V	1-2	13	599	1.021773734	59.35820369	30.18998871
		0.0416703	0.025540			
14007W	1-2	3	378	1.414796348	94.41645498	47.91562566
		0.0414885	0.025970			
14007X	1-2	43	011	1.379353662	98.54296431	49.96115898
		0.0424201	0.028366			
14007Y	1-2	45	248	1.56502639	122.5025212	62.03377379
		0.0406783	0.023371			
14007Z	1-2	59	168	1.225949147	74.38055716	37.80325315
14007A		0.0408122	0.023074			
A	1-2	42	804	1.250791059	71.74773312	36.49926209
14007A		0.0407810	0.021424			
B	1-2	44	614	1.244984529	57.55414712	29.39956582
14007A	1-2	0.0416362	0.022704	1.408120108	68.49031904	34.94921957

Table 9: Continued.

C		35	111			
14007A		0.0408694	0.025804			
D	1-2	52	446	1.26146738	96.94661109	49.10403923
14006A						
D	1-2	0.062	0.037	8.381619458	218.8505301	113.6160748
14007A						
E	1-2	0.054	0.031	4.833272635	150.6548826	77.74407764

Table 10: CB 2-2 surface specimens.

UAL	Core	Asp D/L	Glu D/L	Asp age	Glu age	Mean age
14360A-1	2-2	0.06693702 8	0.031630 549		157.672856 5	
14360A-2	2-2	0.06606597 7	0.030891 821	11.17287684 10.63797591	149.461575 2	84.42286669 80.04977556
14360B	2-2	0.08308987 3	0.037661 447	24.57591388	230.095218 6	127.3355662
14360C	2-2	0.08723207 7	0.043818 387	29.23179756	313.643494 8	171.4376462
14360D	2-2	0.06530687 9	0.031794 367	29.23179756 10.18566041	159.513558 7	84.84960958
14360E	2-2	0.09046561 9	0.045515 02	33.26231774	338.324620 8	185.7934693
14360F	2-2	0.09008339 3	0.037407 866	32.76708625	226.859777 5	129.8134319
14360G	2-2	0.08280359 0.08856159	127 0.040234	24.27429126	289.316016 5	156.7951539
14360H	2-2	0.07546144 8	0.033767 336	30.84570307	263.849224 3	147.3474637
14360I	2-2	5	181 0.039098	17.37038639	182.240701 6	99.80554402
14360J	2-2	0.08378046 0.09071798	026 0.048837	25.31402351	248.734617 9	137.0243207
14360K	2-2	3	976	33.59210834	388.696854 7	211.1444815
14360L	2-2	0.08059166 0.04812695	0.046235 0.023156	22.02841423	349.019517 8	185.523966
14360M	2-2	2	702	2.938042248	72.4727635 5	37.7054029
14360N	2-2	0.07661556 6	0.038675 874	18.35365656	243.202712 9	130.7781847
14360O	2-2	0.05461572	0.030199 895	5.063789388	141.903585 4	73.48368742

Table 10: Continued.

			0.033070		174.094078	
14360P	2-2	0.07605759	238	17.87372792	1	95.98390303
		0.08332886	0.048909		389.811297	
14360Q	2-2	3	557	24.8296627	8	207.3204802
			0.042585		296.147381	
14360R	2-2	0.0908257	048	33.73355721	3	164.9404693
			0.030568		145.915748	
14360S	2-2	0.0725445	675	15.04419745	5	80.47997299
		0.06318632	0.029986		139.601789	
14360T	2-2	4	783	8.988537513	6	74.29516354
			0.049544		399.745413	
14360U	2-2	0.08250337	18	23.96070853	4	211.853061
		0.07167324	0.027885		117.567256	
14360V	2-2	7	417	14.3921765	7	65.97971662
		0.07024566	0.031542		156.685260	
14360W	2-2	1	391	13.36489855	9	85.02507975
		0.06540666	0.030969		150.319444	
14360X	2-2	1	62	10.24438909	6	80.28191685
		0.05826071	0.027257		111.219450	
14360Y	2-2	3	614	6.56381313	5	58.89163183
		0.06937720	0.028054		119.291899	
14360Z	2-2	4	151	12.76439925	5	66.02814937
14360A		0.08197720	0.043419		307.950159	
A	2-2	9	953	23.41781481	5	165.6839871
14360A		0.07858835	0.032160		163.655164	
B	2-2	1	655	20.12018898	4	91.88767667
14360A		0.06886514	0.027124			
C	2-2	5	725	12.41882963	109.889792	61.1543108
14360A		0.07333910	0.032806		171.050394	
D	2-2	6	996	15.65577718	5	93.35308586
14360A		0.07367558	0.036517		215.626155	
E	2-2	8	157	15.91968409	1	115.7729196
14360A		0.08351657	0.035465		202.622101	
F	2-2	7	157	25.03021846	7	113.8261601
14360A			0.040528		267.813915	
G	2-2	0.08004432	408	21.49536608	2	144.6546406
14360A		0.08460990	0.046194		348.414053	
H	2-2	8	987	26.22041123	9	187.3172326
		0.09052833	0.049891		405.216784	
14360AI	2-2	4	103	33.34406482	4	219.2804246
14360A		0.07733657	0.033167		175.218140	
J	2-2	1	058	18.98658198	2	97.10236111
14360A		0.08171087	0.033072		174.124764	
K	2-2	3	884	23.14623406	9	98.63549948
14360A	2-2	0.04783495	0.020190	2.857266541	47.4637535	25.16051004

Table 10: Continued.

L		698		4	
14360A		0.09864821	0.047914	374.422878	
M	2-2	2	042	45.14813213	3
14360A		0.07564310	0.035652	204.912905	
N	2-2	7	174	17.52274377	8
14360A			0.031522		111.2178248
O	2-2	0.05577755	994	5.516379968	156.468241
14360A		0.07221235	0.025095	90.1946794	
P	2-2	5	112	14.79335816	5
14360A		0.05444519	0.024835	87.7630029	
Q	2-2	7	922	4.999308169	8
14360A		0.09358172	0.048154	378.121817	
R	2-2	7	751	37.49420452	4
		0.13964257	0.040935	273.342795	
14360AS	2-2	4	836	151.5886452	3
14360A			0.039757	257.470656	
T	2-2	0.09041952	785	33.2023176	8
14360A		0.07802149	0.035453	202.483202	
U	2-2	3	794	19.60133434	3
14360A		0.05290142	0.026456	103.279517	
V	2-2	4	646	4.43764259	2
14360A		0.07429132	0.030012	53.8585799	
W	2-2	7	153	16.41029699	139.875162
14360A		0.09135354	0.059572	78.14272951	
X	2-2	7	301	569.332535	
14360A		0.08763961	0.041435	301.8825922	
Y	2-2	4	449	34.43264909	
14360A			0.027020	154.9498262	
Z	2-2	0.28972393	851	29.72017644	
14360B		0.07675791	0.032915	280.179476	
A	2-2	7	361	1881.464435	4
14360B		0.07209460	0.039838	995.1591485	
B	2-2	4	337	172.301114	
14360B		0.05036487	0.027871	95.3892932	
C	2-2	1	164	258.544806	
14360B		0.07583991	0.040209	136.6249558	
D	2-2	3	985	263.521912	
14360B		0.04555301	0.021480	140.6053637	
E	2-2	7	084	58.0183302	
14360B		0.09255164	0.048415	30.14235685	
G	2-2	2	273	382.140960	
14360B				209.0987021	
H	2-2	0.057	0.027	108.646275	
				57.33219071	